Interparticle friction and Rheology of Dense suspensions

PhD candidate:

Anh Vu NGUYEN LE

Supervisor :

Annie Colin

Jury members:

Hugues BODIGUEL

Frédéric BLANC

Michel CLOITRE

Laurence TALINI

Guillaume OVARLEZ

Outline

- **BACKGROUND ON THE RHEOLOGY OF DENSE SUSPENSIONS:**
  Important but not well-understood role of **particle friction μ_p.**
- **AIM OF MY THESIS:**
  Evidencing the relation between μ_p and **rheology**.
- **MATERIALS UNDER SCRUTINY:**
  Polystyrene **(PS) beads** in various **matrix fluid.**
- **METHODS OF CHARACTERIZATION:**
  Tuning-fork force microscope (TFM) and **Rheometry.**
- **RESULTS AND DISCUSSIONS:**
  How different μ_p **profiles** explains different **rheological behaviors.**
- **CONCLUSION AND OUTLOOKS:**
  The importance of studying μ_p in **rheology.**

BACKGROUND

on the rheology of dense suspensions

What is a suspension?

‘Solid particles suspended in a liquid’

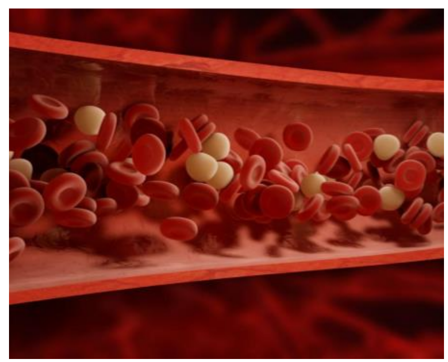

Credit: Google image
Handbook of Flexible Organic Electronics

Great interest in studying suspensions’ flow

Simplification:

Smooth hard spheres

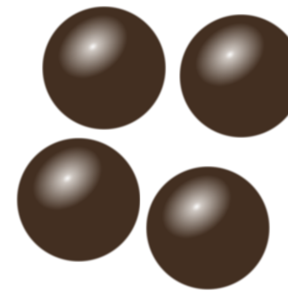

+

Newtonian fluid

Dense suspension = high **solid fraction** $\phi = \frac{V_{solid}}{V_{total}}$

What is Rheology?

'Study of flow'. How?

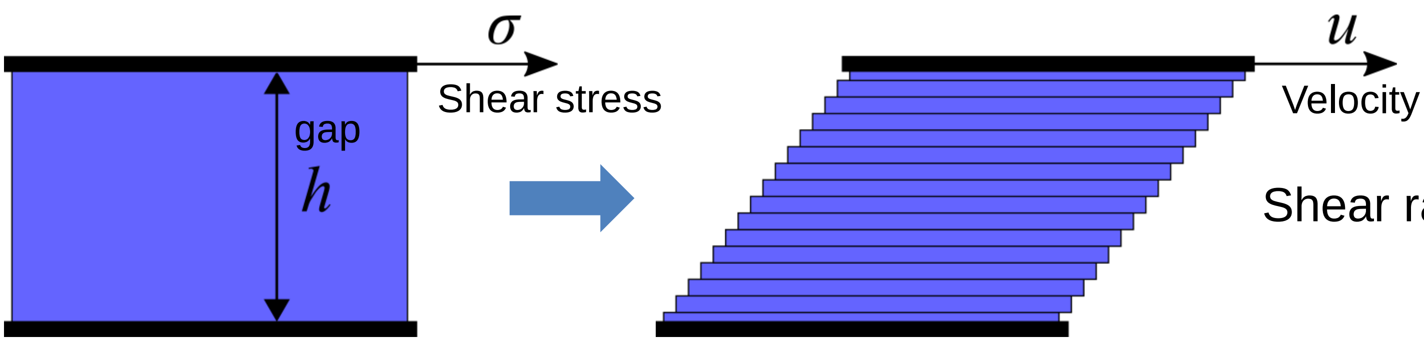

Shear rate: $\dot{\gamma} = \frac{u}{h}$

Viscosity: $\eta = \frac{\sigma}{\dot{\gamma}}$

Flow curves

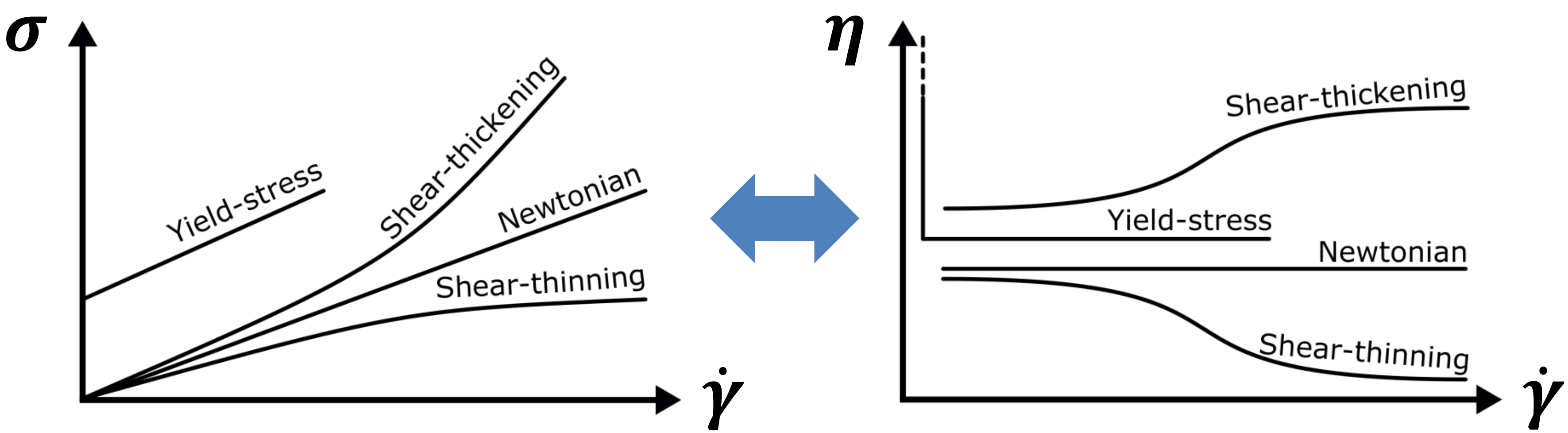

Non-Newtonian behaviors

An example: Flow curves of PVC particles suspended in DINCH plasticizer

Chatté et al., Soft Matter (2018)

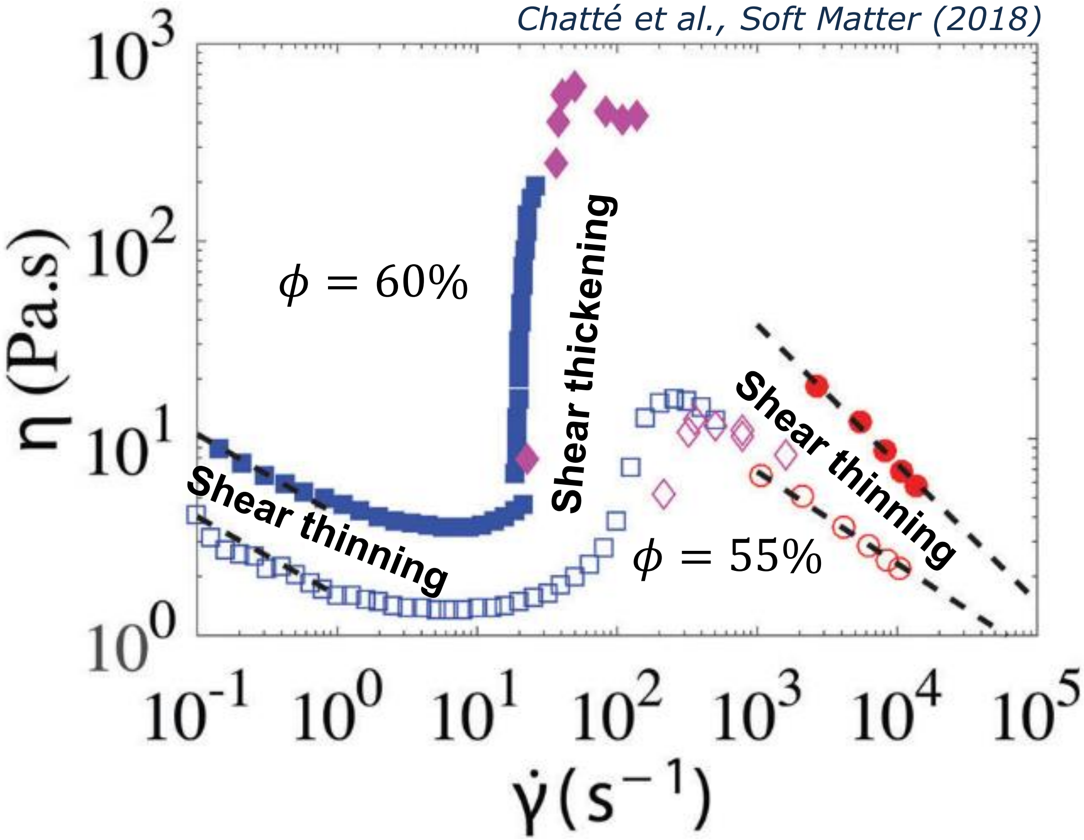

Consequences:

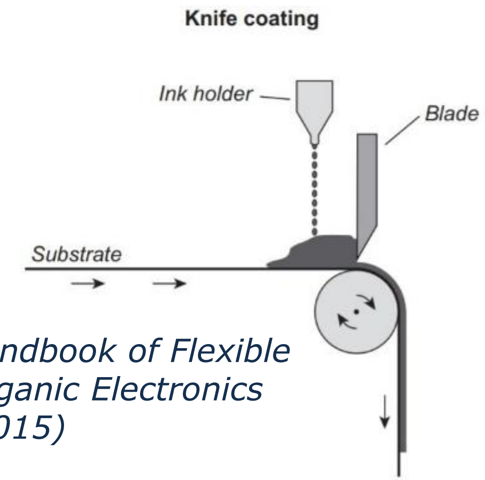

Handbook of Flexible Organic Electronics (2015)

Credit: medium.com

What is the current understanding on non-Newtonian behaviors?

Dimensional analysis

Rheological parameters

- $\boldsymbol{d}$: particle diameter
- $\boldsymbol{\rho_p}$: particle density
- $\boldsymbol{n}$: number concentration
- $\boldsymbol{\rho_f}$: fluid density
- $\boldsymbol{\eta_f}$: fluid viscosity
- $\dot{\boldsymbol{\gamma}}$: shear rate
- $\boldsymbol{k_B T}$: thermal energy

7 variables with 3 units:

$[\mathrm{kg}]$ $[\mathrm{m}]$ $[\mathrm{s}]$

Buckingham π theorem

Only 7 – 3 = 4 dimensionless variables left:

$Re = \frac{\rho_f \dot{\gamma} d^2}{\eta_f}$	$Pe = \frac{3\pi \eta_f \dot{\gamma} d^3}{4 k_B T}$	$Sh = \frac{\eta_f \dot{\gamma}}{\Delta\rho g d}$	$\phi = n \frac{\pi}{6} d^3$
Viscous vs Inertial	Viscous vs Brownian	Viscous vs Gravity	Solid fraction

Density-matched: $Sh \gg 1$

Non-Brownian: $Pe \gg 1$

$\Rightarrow$ $\eta_s = f_\eta(Re, \phi)$

with $\boxed{\eta_s = \eta/\eta_f}$

2 flow regimes:

Re ↑ / Pe →			
	Brownian, high Reynolds	Non-Brownian, high Reynolds	Inertial regime
	Brownian, low Reynolds	Non-Brownian, low Reynolds: Newtonian-like	Viscous regime

Inertial regime (high Re)

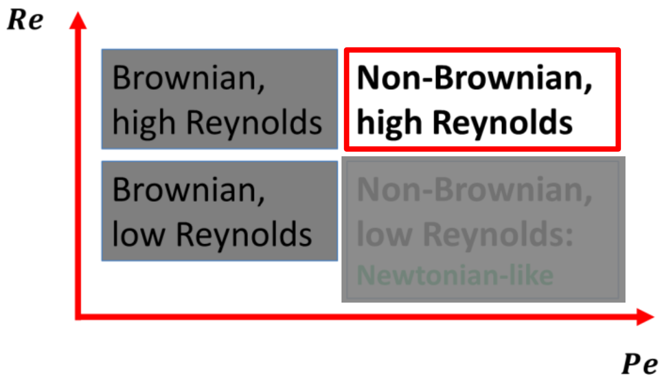

Inertia dominates:

Only 4 particle-related parameters:

$\rho_d, d, n, \dot{\gamma}$ ➔ 1 dimensionless number

The paradigm of dense granular matter:

Da Cruz et al., Phys. Rev. E (2005)

$$I = d\dot{\gamma}\sqrt{\frac{\rho_p}{P^P}}$$

2 behavior laws:

$$\begin{cases} \phi = g(I) \\ \sigma = f(I)P^P \end{cases} \quad \rightarrow \quad \sigma = f\left(g^{-1}(\phi)\right)\frac{\rho_p d^2}{\left(g^{-1}(\phi)\right)^2}\dot{\gamma}^2$$

$\sigma = A(\phi)\dot{\gamma}^2$: if ϕ is constant, σ varies as a function of $\dot{\gamma}^2$.

At **high Re**: Suspensions will **shear thicken.**

Viscous regime (low Re)

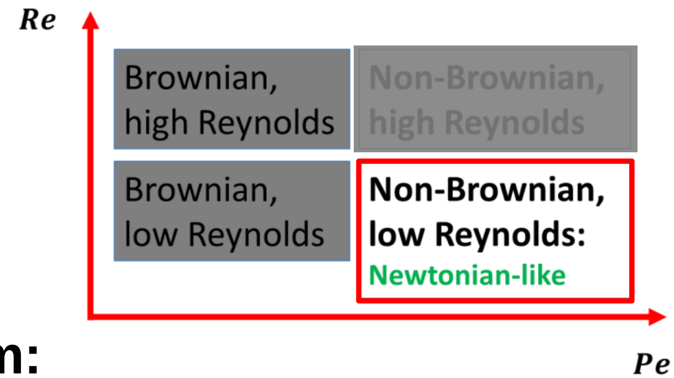

Viscous effects dominate:

Only 4 fluid-related parameters:

$d,\ \eta_f,\ n,\ \dot{\gamma}$ ➔ 1 dimensionless number

Borrowing from granular-matter paradigm:

Boyer et al., PRL (2011)

$$\boxed{I_v = \frac{\eta_f\,\dot{\gamma}}{P^P}}$$

2 behavior laws:

$$\begin{cases} \phi = g(I_v) \\ \sigma = f(I_v)P^P \end{cases} \quad \rightarrow \quad \sigma = f\left(g^{-1}(\phi)\right)\frac{\eta_f}{g^{-1}(\phi)}\dot{\gamma}$$

$\boxed{\sigma = \eta_s(\phi)\,\eta_f\dot{\gamma}}$: if ϕ is constant, σ will be proportional to $\dot{\gamma}$.

At **low** Re**:** Suspensions should behave as Newtonian fluid**.**

Background

Dependence $\eta_s(\phi)$ on μ_p

Chèvremont et al., Phys. Rev. Fluids (2019)

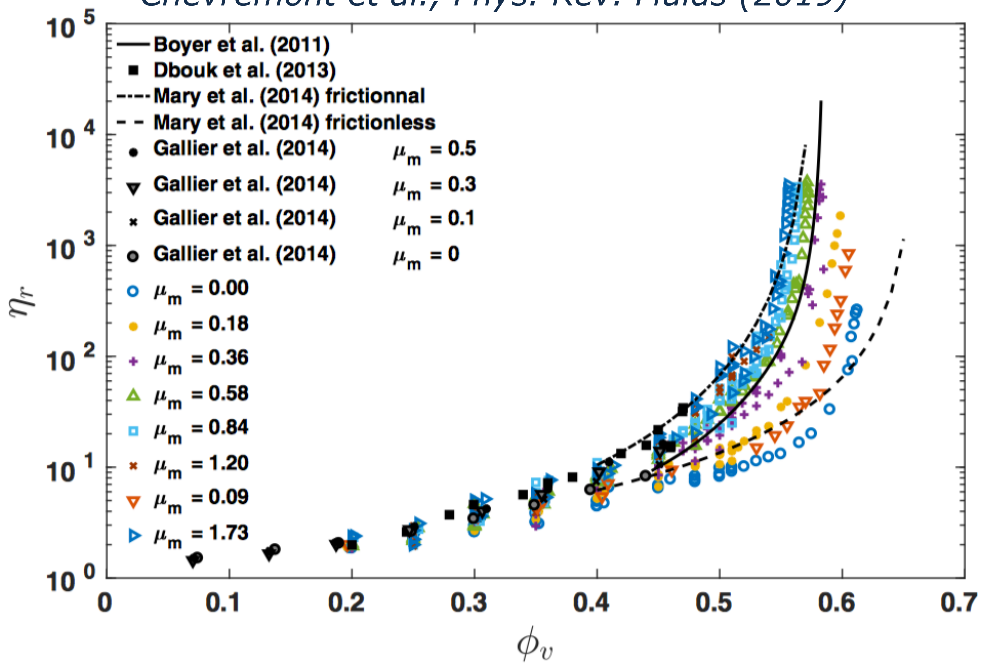

Guazzelli & Pouliquen, JFM (2018)

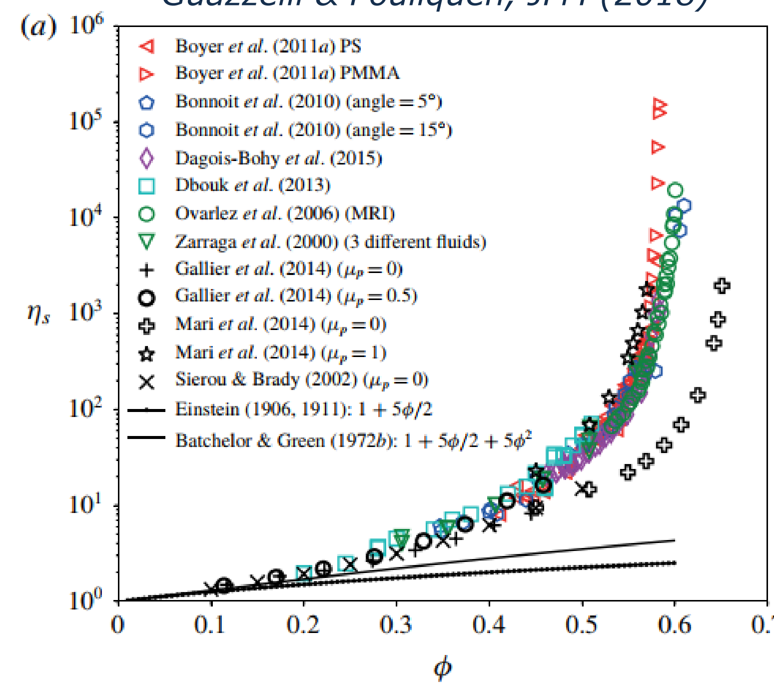

$\boldsymbol{\eta_s(\phi)}$ **curve** shifts leftward when **particle friction coefficient $\boldsymbol{\mu_p}$** increases.

The role of $\boldsymbol{\mu_p}$ is crucial
but experimental data on $\boldsymbol{\mu_p}$ is still lacking.

Shear Thickening

Explanation: **Shear-induced transition**
from Low-friction profile (soft/no contact)
to High-friction profile (hard contact)

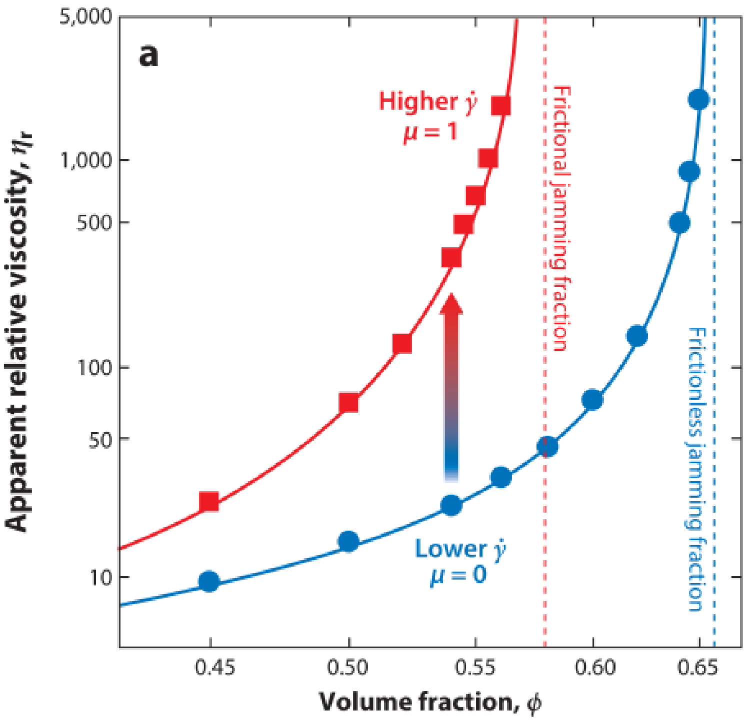

Morris, Annu. Rev. Fluid Mech. (2020)
Mari et al., J. Rheol. (2011)

$$\mu_p = \frac{Friction}{Load}$$

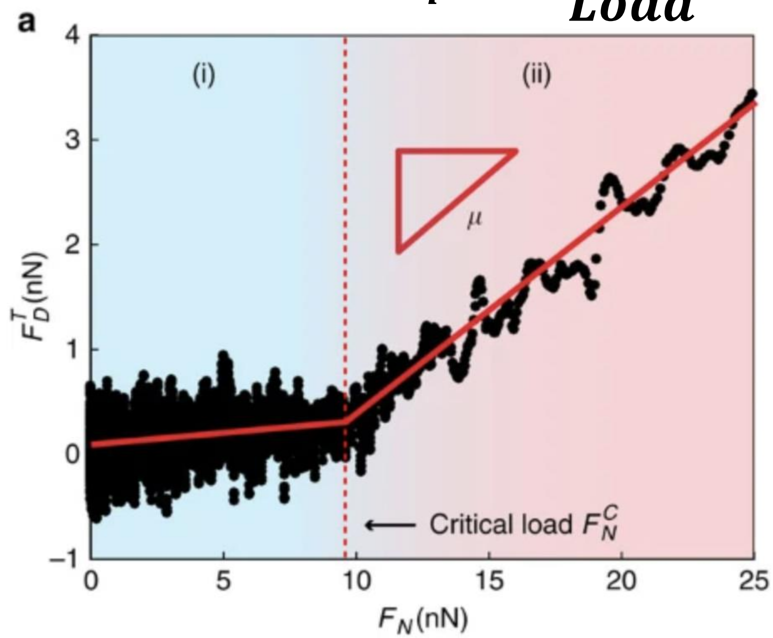

Comtet et al., Nat. Comm. (2017)

Background

Shear Thinning

Explanation: **Decrease of μ_p** with **increasing normal load F_n**

Chatté et al., Soft Matter (2018)

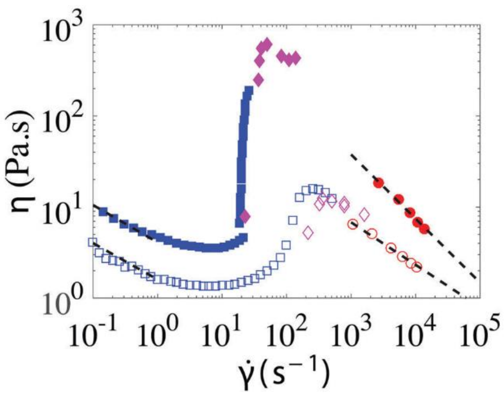

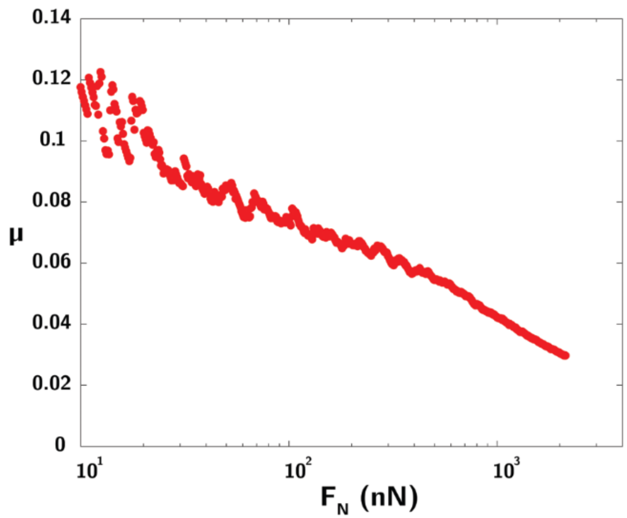

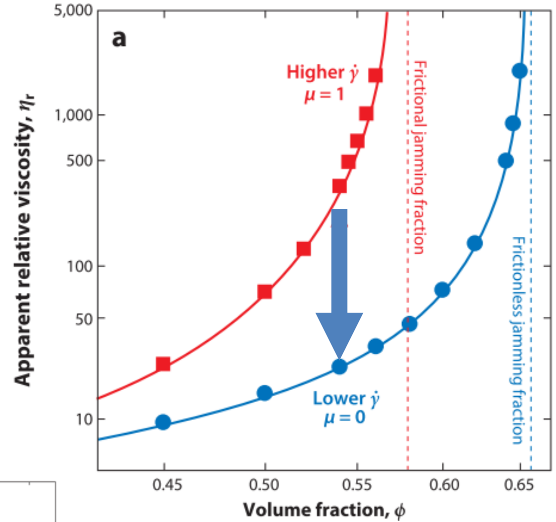

Arshad et al., Soft Matter (2021)

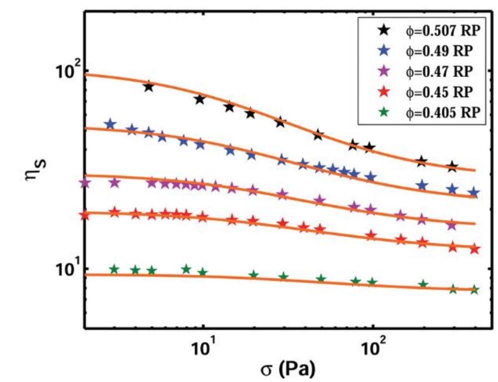

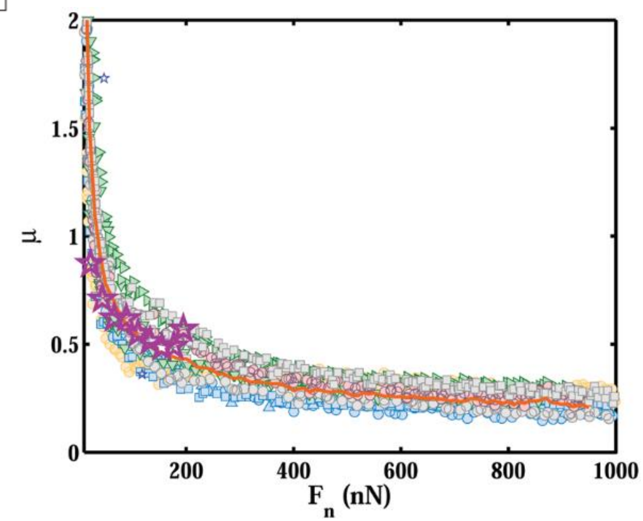

Open questions

1. Is something else missing in the rheological description?

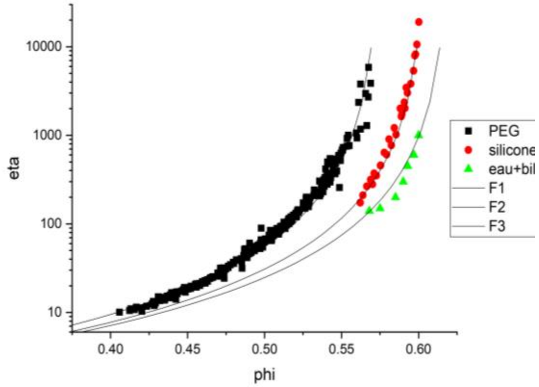

- Well-established theoretical framework for suspension of smooth hard non-Brownian spheres.
- But lack of experimental data on μ_p to explain their rheology.

Ovarlez et al.: How to explain the lateral shift of the $\eta_s(\phi)$ curves as a function of the solvent?

2. How does shear-thickening occur even in the frictionless state?
3. How do shear-thickening suspensions flow in the frictional state?

Aim of my thesis

Response

2. FRICTIONLESS SHEAR-THICKENING OCCURS AT HIGH Re:

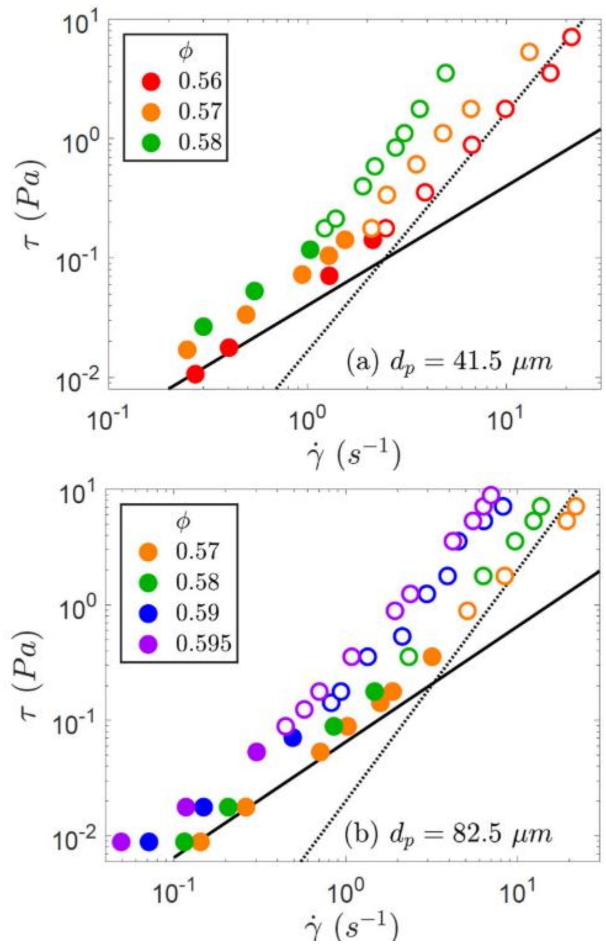

Madraki et al., JoR (2020)

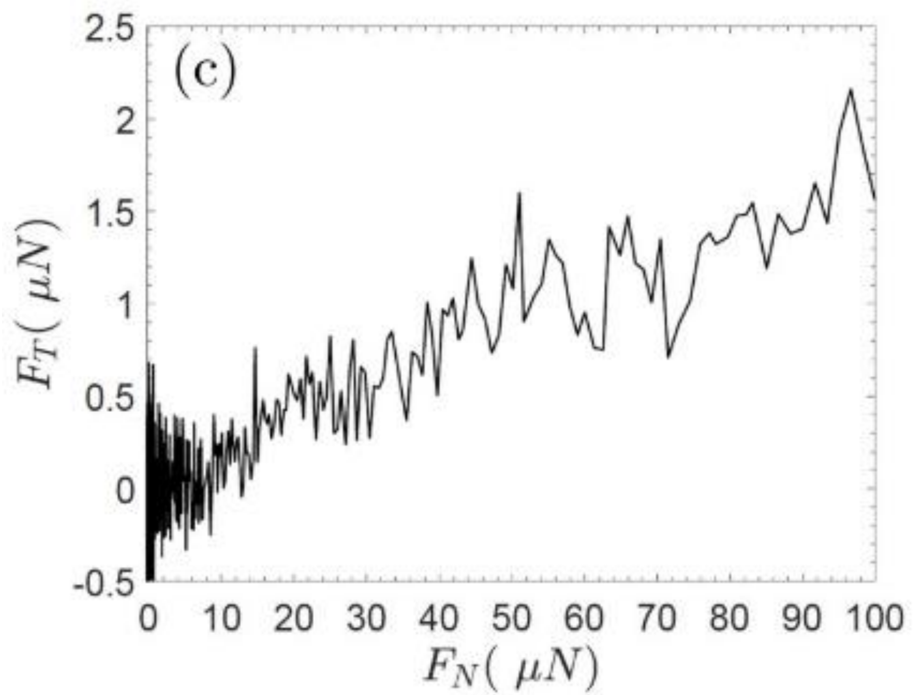

Viscous-to-inertial transition can occur before repulsive-to-frictional transition.

Response

3. INSTABILITY DURING SHEAR-THICKENING TRANSITION:

Shear fluctuations

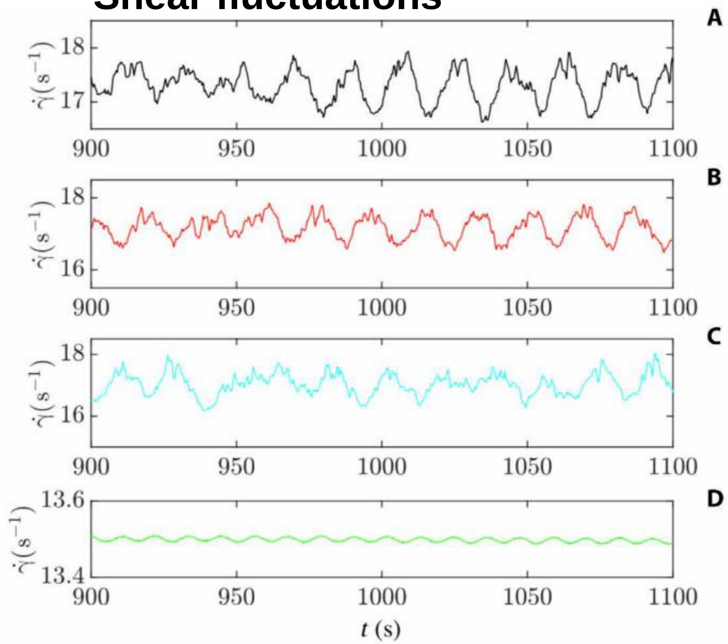

Density fluctuations

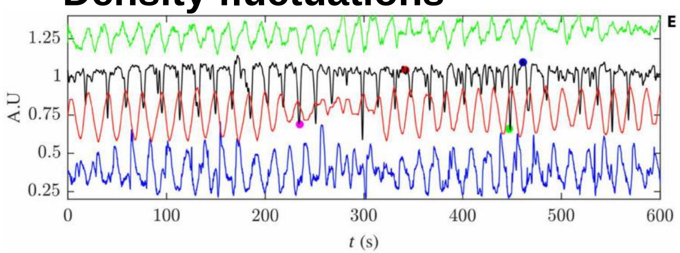

Ovarlez et al., Sci. Adv. (2020)

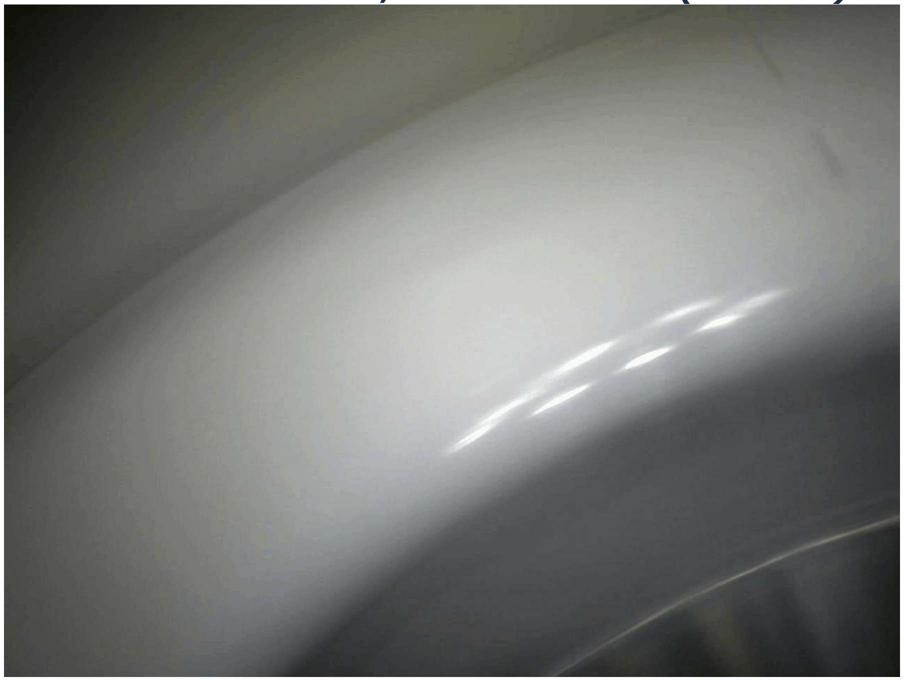

Density waves propagating in the velocity direction generate shear instabilities.

Response

1. THE ROLE OF SOLVENT ON THE RHEOLOGICAL BEHAVIORS :

What is the influence of solvent on the $\eta_s(\phi)$ curves?

What is the description at the microscopic level (F_N^C, F_T^D, and μ_p)

How the dependence of μ_p on normal load results in shear thinning?

Materials
under scrutiny

Particle cleaning

Polystyrene (PS) spheres, $R = 20\ \mu\mathrm{m}$

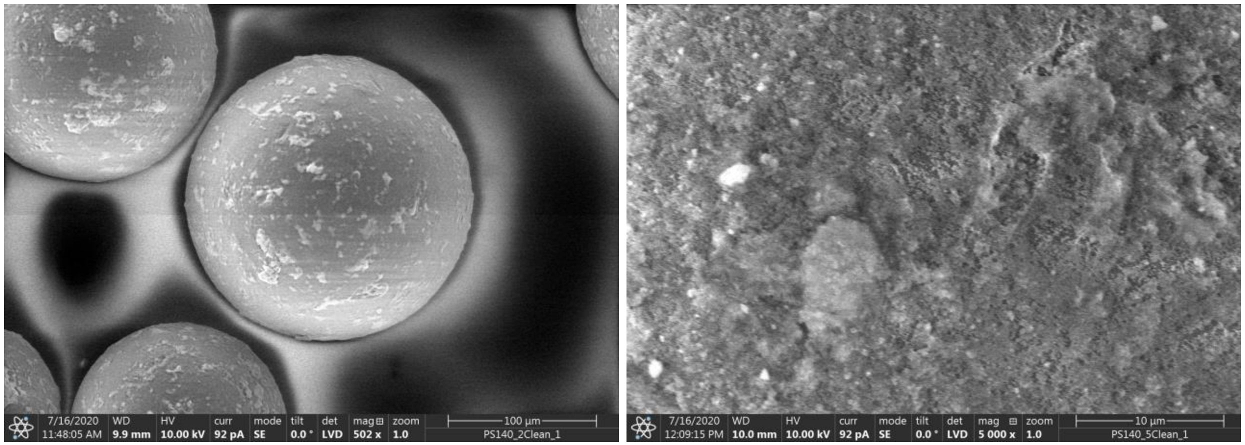

SEM micrograph of washed PS spheres

Washing process:

- Sonicate the raw beads in deionized water.
- Replace regularly the bathwater.
- Filter out the ‘creamed’ beads. (Pickering emulsion).
- Dry at 70°C until becoming powder-like.

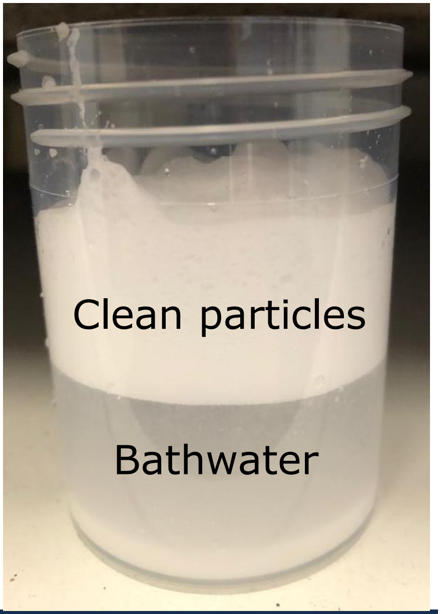

Suspension preparation

Solvents

NaI solution, $\eta_f \approx 1\ \mathrm{mPa\ s}$
(density-matched)

Silicone oil, $\eta_f \approx 20\ \mathrm{mPa\ s}$

PEG, $\eta_f \approx 2000\ \mathrm{mPa\ s}$
(Poly(ethylene glycol-ran-propylene glycol) mono-butyl ether)

$\left.\begin{matrix} \\ \\ \end{matrix}\right\}$ **Newtonian fluids**

Preparation protocol:

- Weigh the particles.
- Add the solvent.
- Homogenize the mixture
- Degas the mixture using vacuum (if not water-based)
- Homogenize the mixture before each rheometric measurement.

METHODS
of characterization

Tuning-fork force microscope (TFM)

2 setups for 2 force scales:

With aluminum tuning fork (TF):

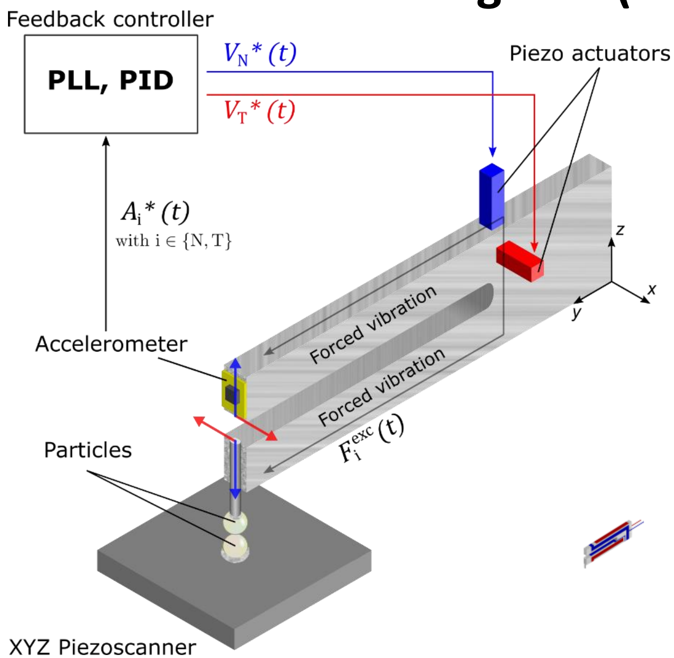

Prongs' dimension:

$L = 75$ mm, $W = 6.8$ mm,

$T = 12$ mm

With quartz tuning fork (TF):

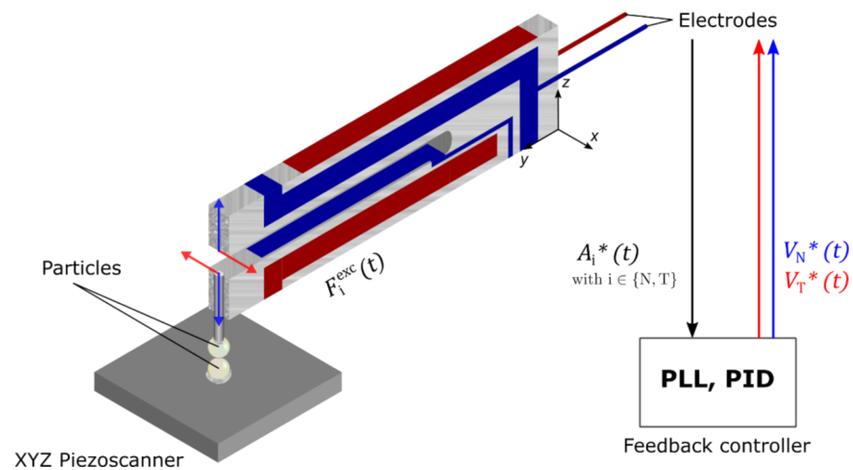

Prongs' dimension:

$L = 3.75$ mm, $W = 0.34$ mm,

$T = 0.6$ mm

Quartz TF is 20 times smaller than aluminum TF.

Principle of TFM

Models:

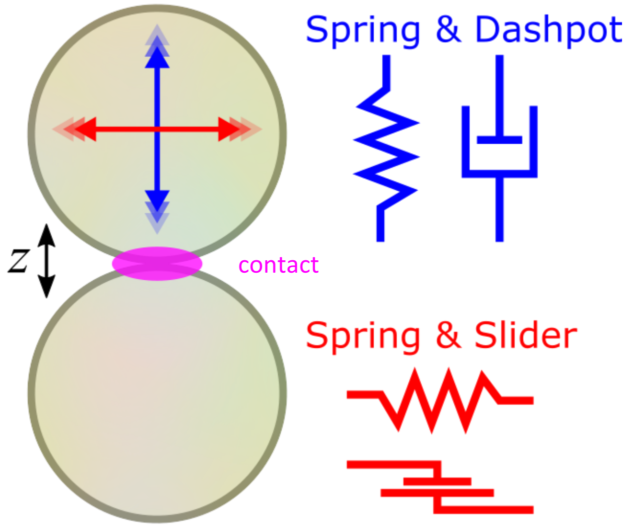

WITHOUT interactions between particles:

- Resonate at a frequency f_0
- Require an excitation voltage E_0 (to maintain a constant oscillation amplitude A)

WITH interactions between particles:

- Resonate at a frequency $f(z)$
- Require an excitation voltage $E(z)$ (to maintain the same amplitude A)

F_N^C: Normal conservative force (elastic force)

$$F_N^C(z) = -2\frac{k_0^N}{f_0^N}\int \delta f^N(z)\,\mathrm{d}z$$

F_T^D: Tangential dissipative force (frictional force)

$$F_T^D(z) = \frac{4}{\pi}C^T\left(E^T(z) - E_0^T\right)$$

2 modes are decoupled

Determination of $z = 0$

$z = z_{\mathrm{raw}} - z_0$. z_0 is the raw separation where E_T rises out of the noise.

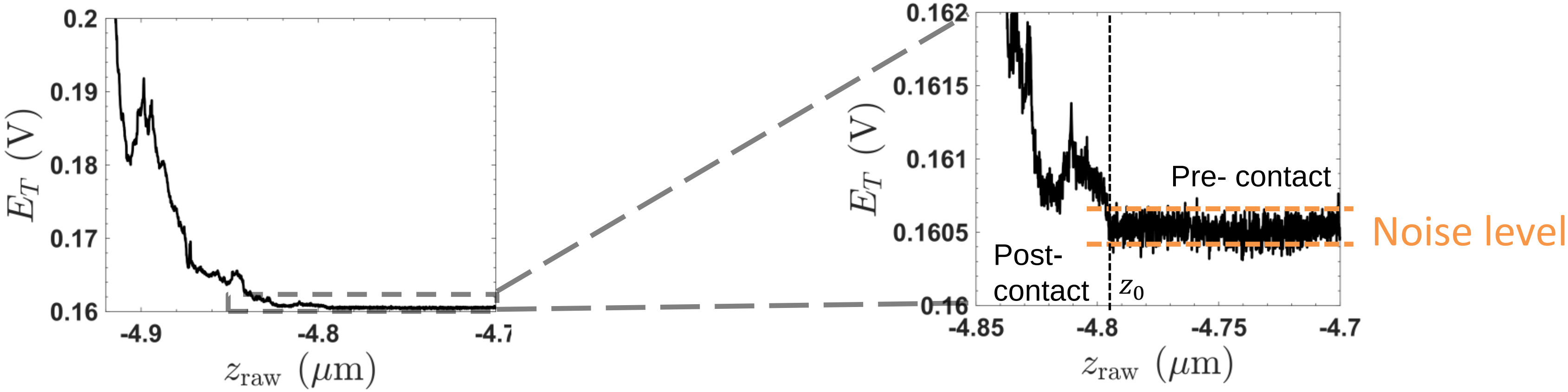

Incorrect $z = 0$ results in artifacts on repulsive force before contact, but no effect on μ_P.

Thermal drift correction: for $\delta F_N^C(z)$ and $E_T(z)$

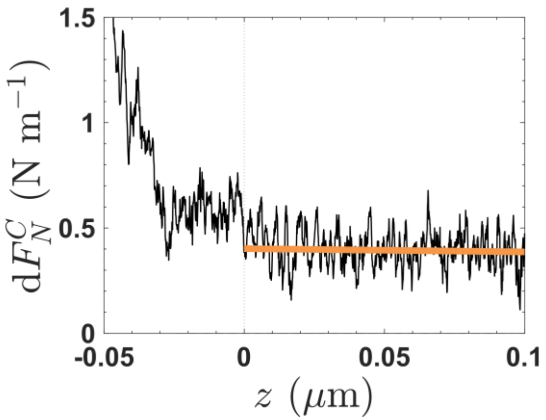

- Apply a linear fit for the signals before contact.
- Subtract the fit value from raw data.
- Calculate the forces using the resulting value.

Raw signal of TFM (air)

Aluminum TF:

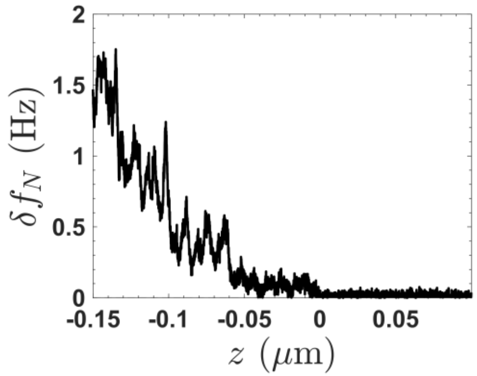

Sensitivity:

$$s_N^C = \frac{2k_0^N}{f_0^N}$$

$$\approx 700\,\mathrm{N\,m^{-1}\,Hz^{-1}}$$

Noise level

$$\approx 0.01\,\mathrm{Hz}$$

Minimal stiffness shift $\approx 7\ \mathrm{N\,m^{-1}}$

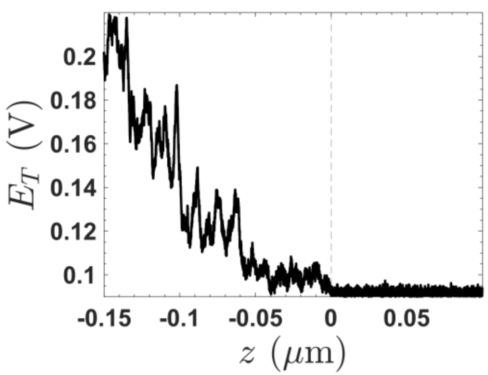

Sensitivity:

$$C_T = \frac{k_0^T}{Q_0^T} C_{\mathrm{drive}}^T$$

$$\approx 30\,\mu\mathrm{N\,V^{-1}}$$

Noise level

$$\approx 1\,\mathrm{mV}$$

Minimal force $\approx 30\ \mathrm{nN}$

More stable versus high normal load

Quartz TF:

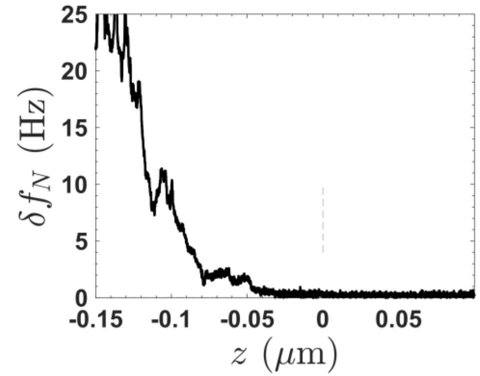

Sensitivity:

$$s_N^C = \frac{2k_0^N}{f_0^N}$$

$$\approx 1\,\mathrm{N\,m^{-1}\,Hz^{-1}}$$

Noise level

$$\approx 0.1\,\mathrm{Hz}$$

Minimal stiffness shift $\approx 0.1\ \mathrm{N\,m^{-1}}$

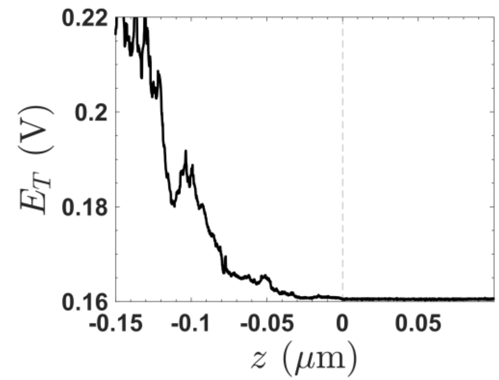

Sensitivity:

$$C_T = \frac{k_0^T}{Q_0^T} C_{\mathrm{drive}}^T$$

$$\approx 10\,\mu\mathrm{N\,V^{-1}}$$

Noise level

$$\approx 0.1\,\mathrm{mV}$$

Minimal force $\approx 3\ \mathrm{nN}$

More sensitive to small forces

Force measurement (air)

Aluminum TF:

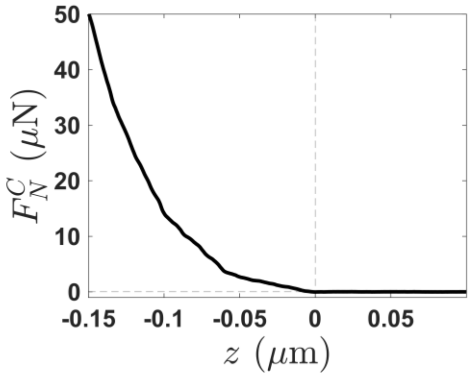

Normal load (FCN):

$$F_N^C = s_N^C \int \delta f^N(z)\,\mathrm{d}z$$

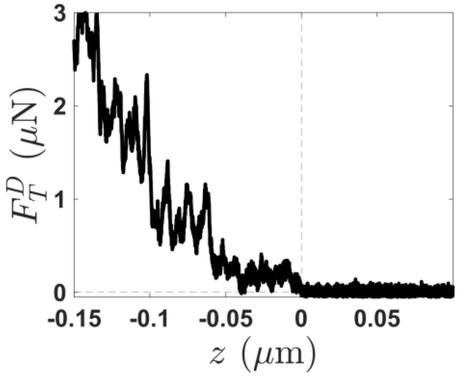

Tangential friction (FDT):

$$F_T^D = \frac{4}{\pi} C_T \left(E^T(z) - E_0^T \right)$$

Quartz TF:

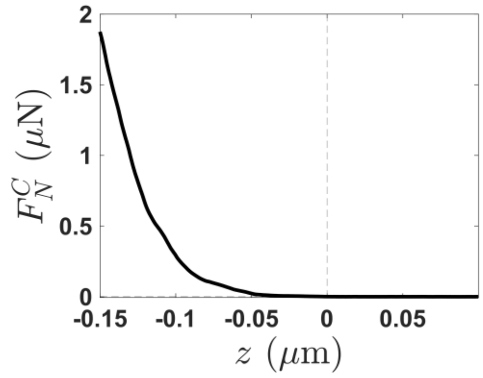

Normal load (FCN):

$$F_N^C = s_N^C \int \delta f^N(z)\,\mathrm{d}z$$

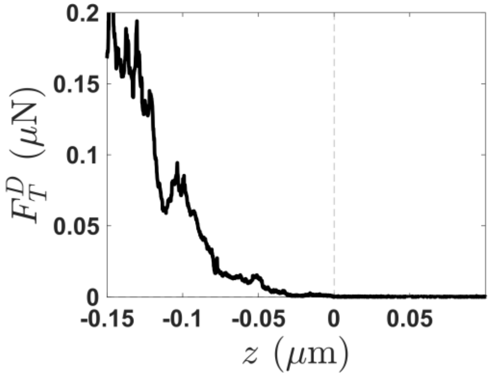

Tangential friction (FDT):

$$F_T^D = \frac{4}{\pi} C_T \left(E^T(z) - E_0^T \right)$$

Raw signal from quartz TF (solvents)

NaI solution (Quartz)

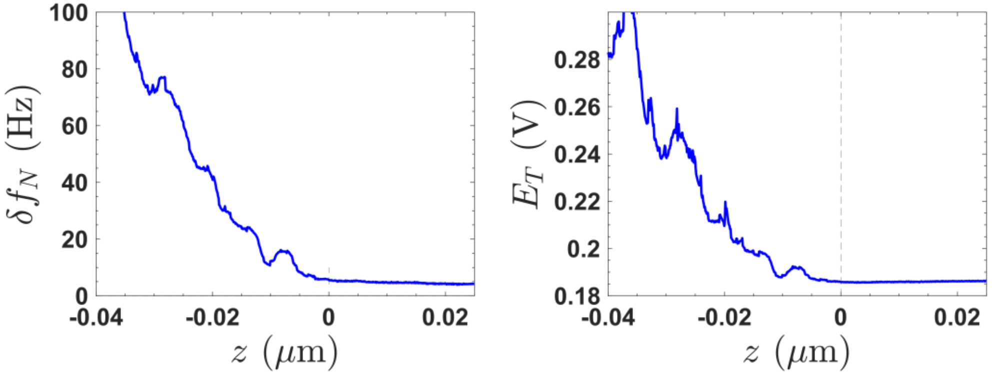

Silicone oil (Quartz)

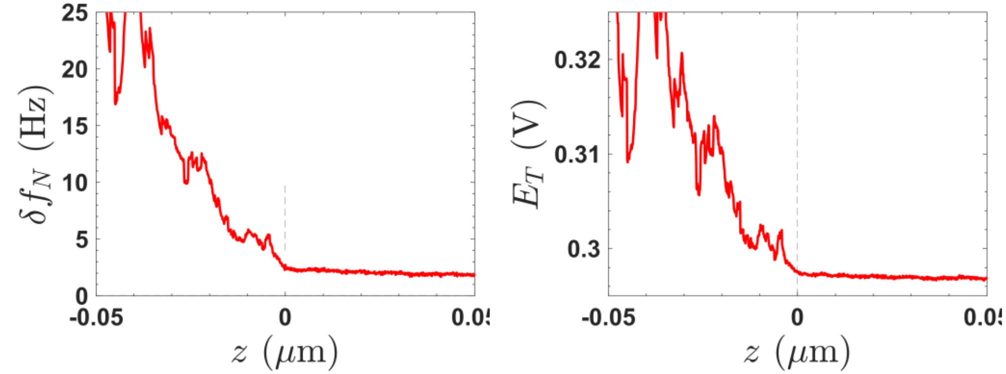

PEG (Aluminum)

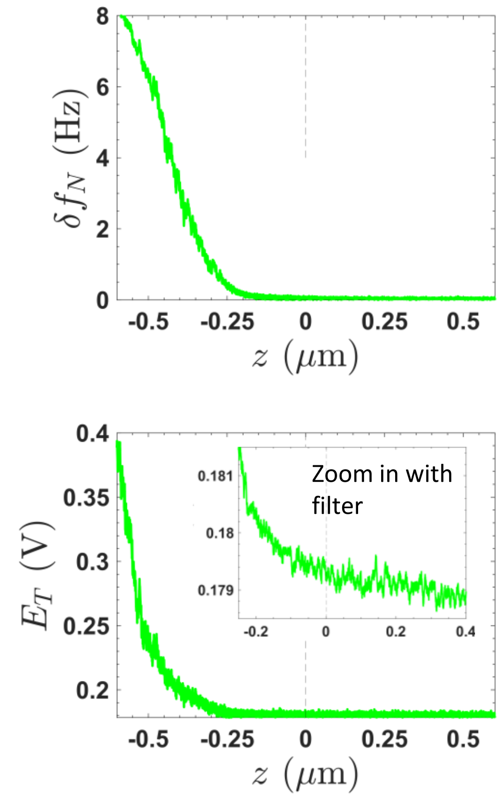

No significant change in noise level at $\eta_f \leq 20$ mPa s.

For $\eta_f = 2000$ mPa s, $E_T(z)$ is roughly 2 times noisier.

Noise and measure bias

Possible source of noise:

- **High humidity**

→ Counteracted by placing dehydrator in the measuring chamber.

- **Acoustic and mechanical vibration**

→ Counteracted by using acoustic box, anchor, and anti-vibration table.

- **Electronic noise**

→ Negligible compare the force scale of interest.

- **Thermal noise** (negligible at our scale).
- **Noise from motors** inside the chamber (negligible at our scale).

Possible bias:

- Starting and ending point of the linear fit for the thermal drifts.

Rheometry

Principe:

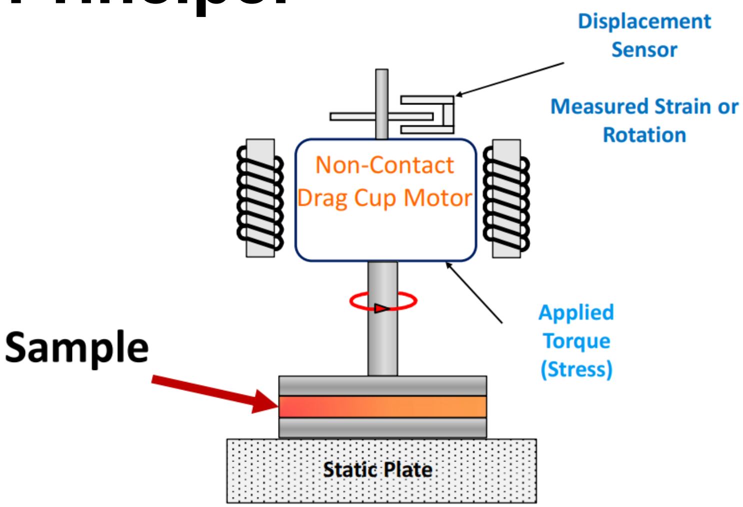

TA instruments (2019)

Geometries:

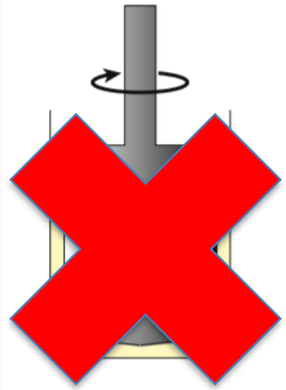

Severe migration to the bottom and the exterior

Not suitable for large particles

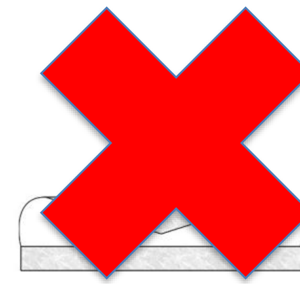

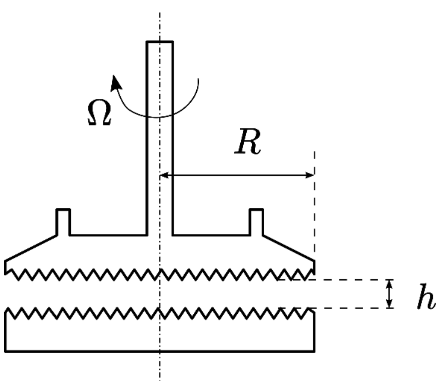

Help to avoid wall slip. No migration.

Might have sedimentation and drainage problem.

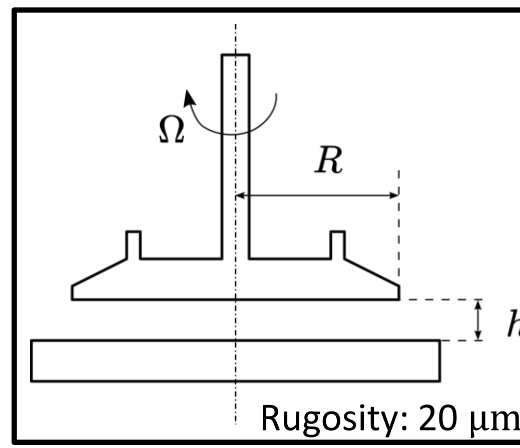

Results & Discussion

Contact force profiles

Silicone oil

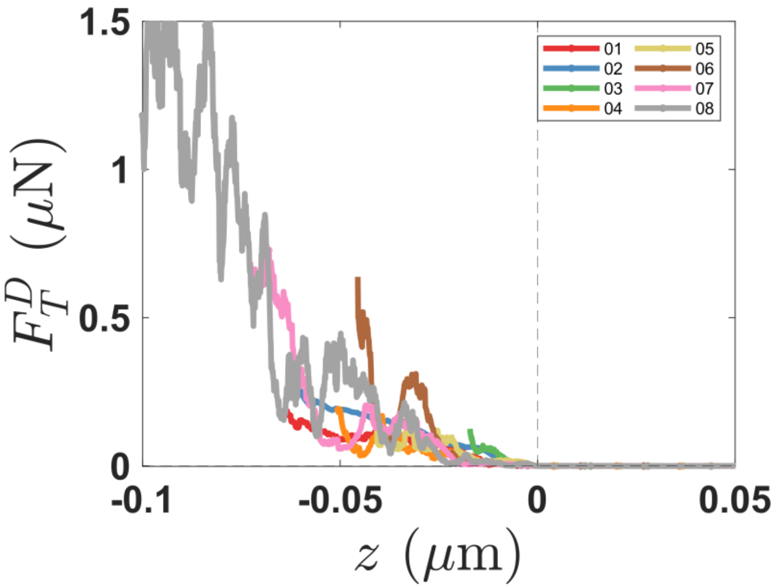

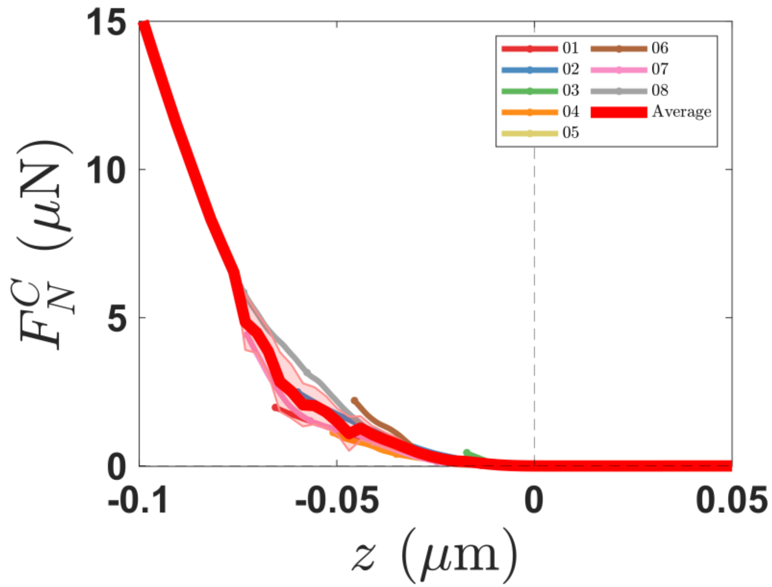

$F_N(z)$ **model:** $F_N^C = f(z, E_0, h_r)$

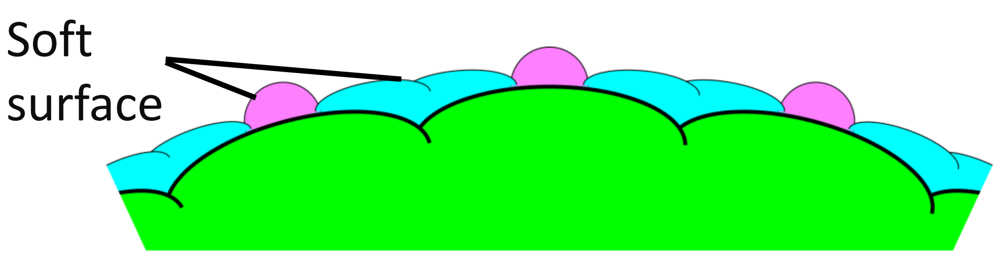

z	E_0	h_r
0 nm - 15 nm	1 GPa	15 nm
15 nm - 50 nm	1 GPa	90 nm
50 nm - center	3 GPa	530 nm

Contact force profiles

Silicone oil

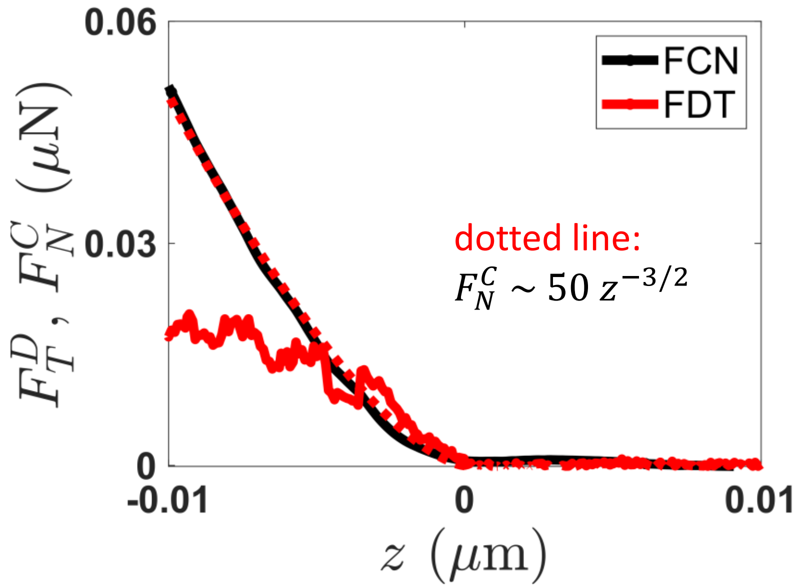

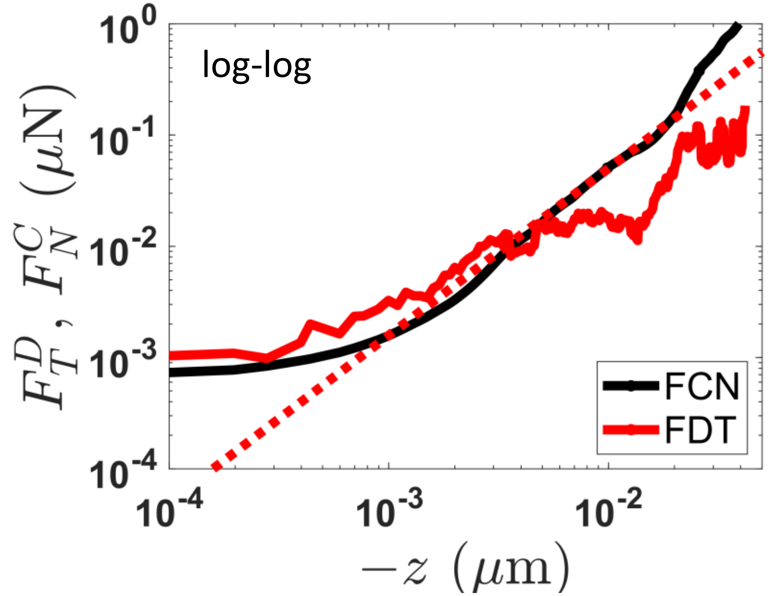

No sign of repulsive force

→ Quasi-unstable suspension (with very low yield stress)

Close to $z = 0$, Hertz model with either
low contact radius (from asperities) or low Young modulus.

Contact force profiles

NaI solution

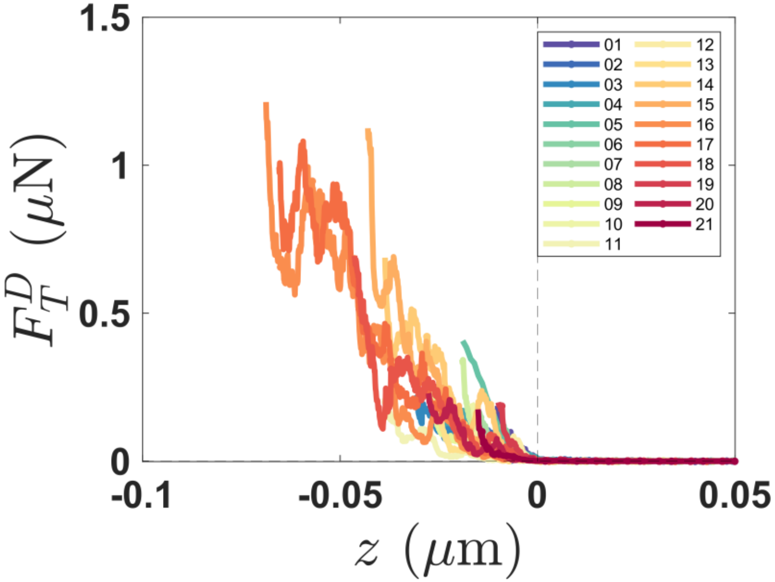

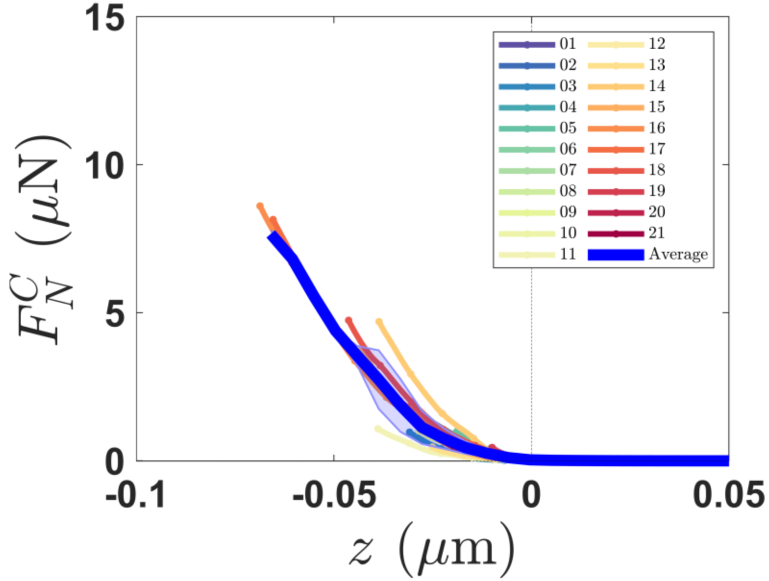

Presence of repulsive forces.

Repulsion added to the force profile after contact.

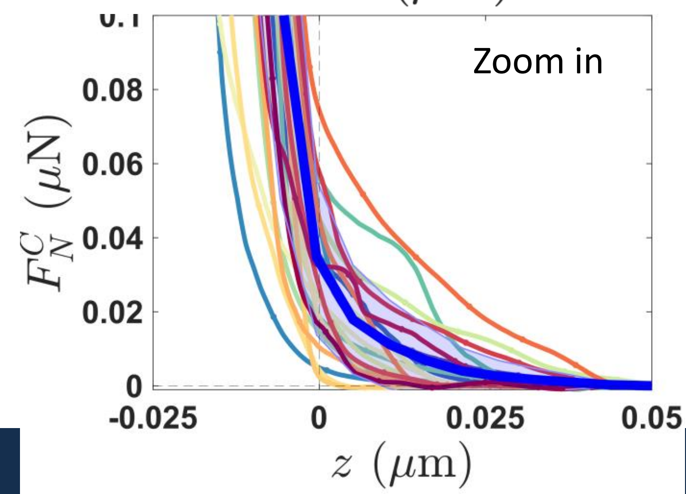

Contact force profiles

NaI solution

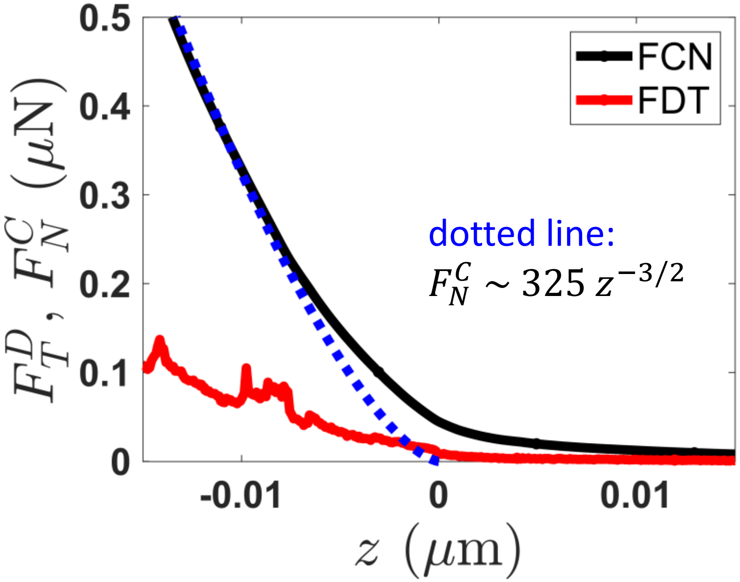

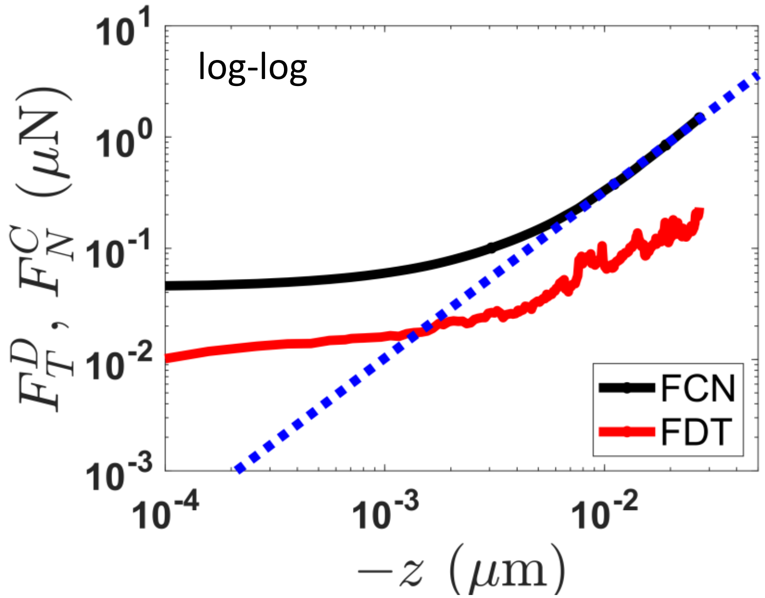

Debye length $\lambda_D = 0.4\ \mathrm{nm}$ for solution of $I = 0.5136\ \mathrm{M}$

→ Not ionic repulsion. Must be of steric origin.

At high overlap, Hertz model with the Young modulus of PS.

Results & Discussion

Contact force profiles

PEG

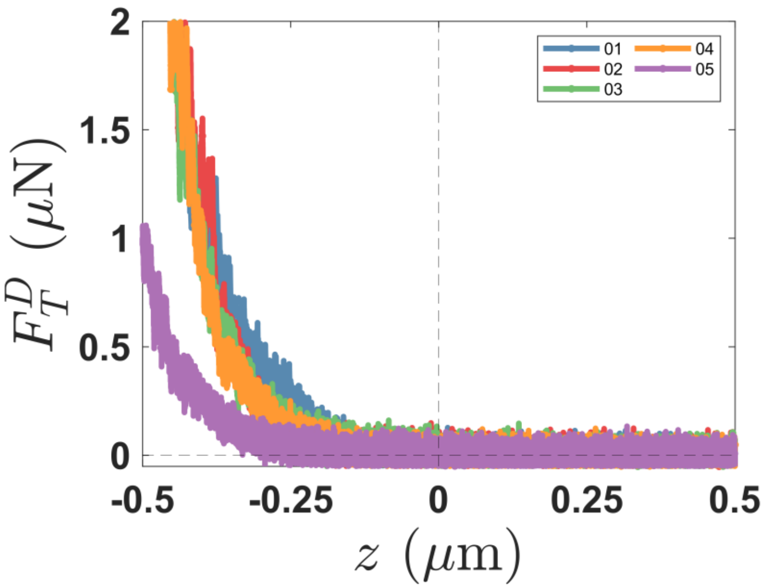

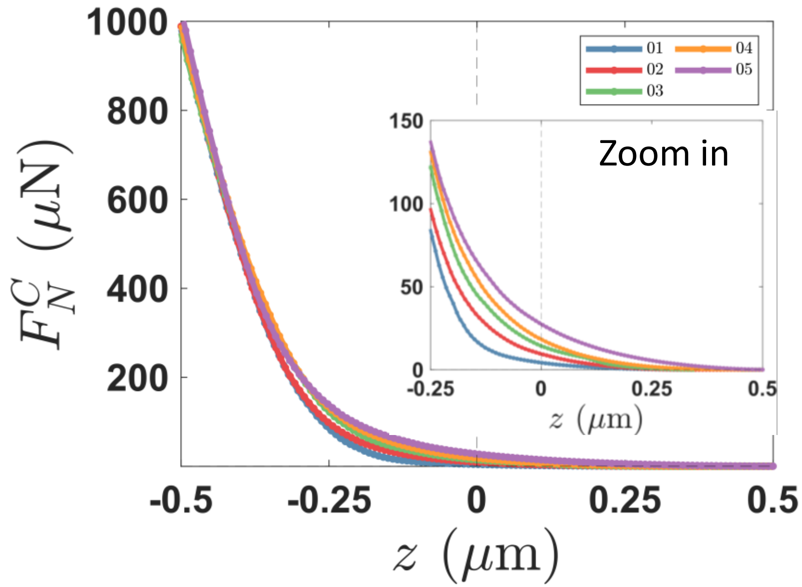

PS particles swell in PEG.

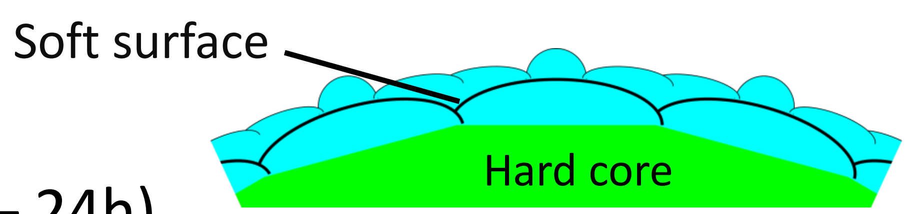

Swelling increases with the submerged duration (1h – 24h).

Swelling modifies the solid fraction: $\phi_{\mathrm{eff}} = \beta\, \phi$.

Contact force profiles

PEG

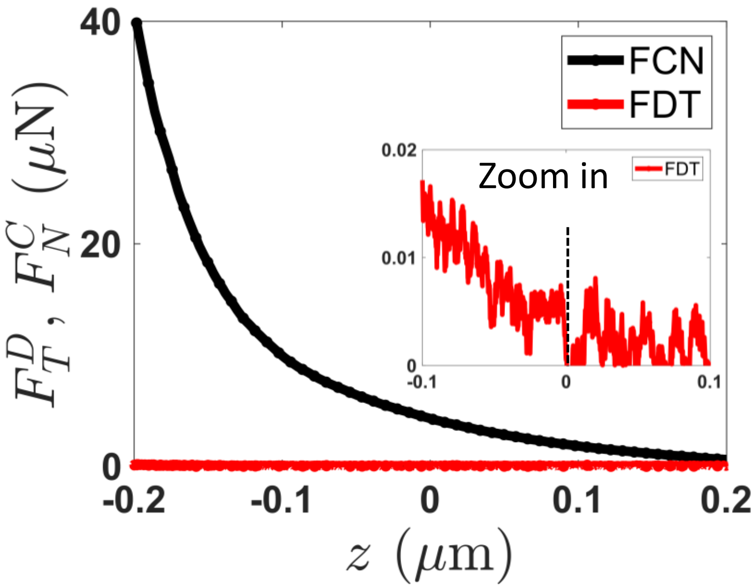

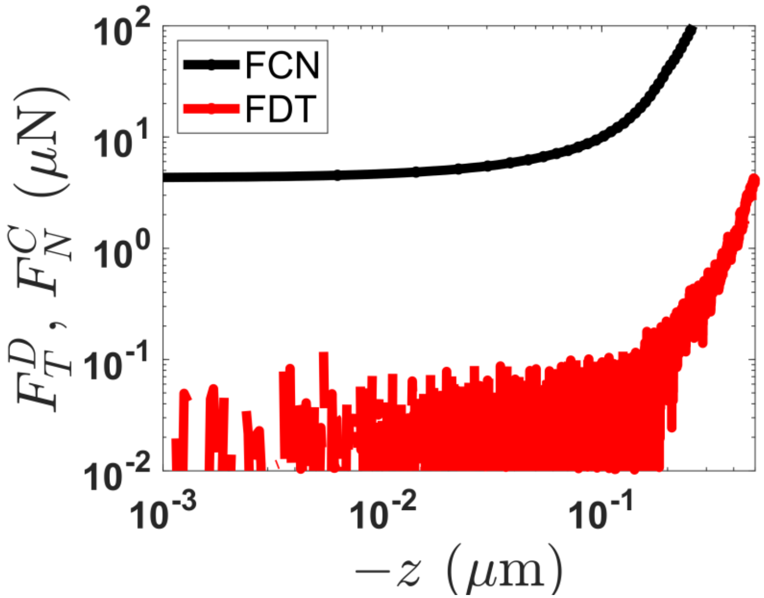

$z = 0$ is determined by the same method as before.

Normal load are more 2 orders of magnitude higher than Friction.

$\mu_p(F_N)$-profile in oil

Silicone oil

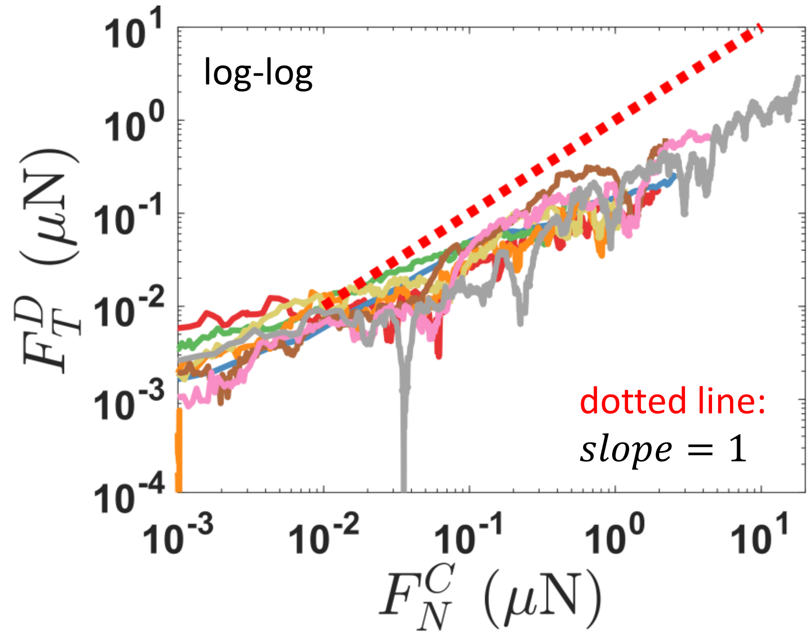

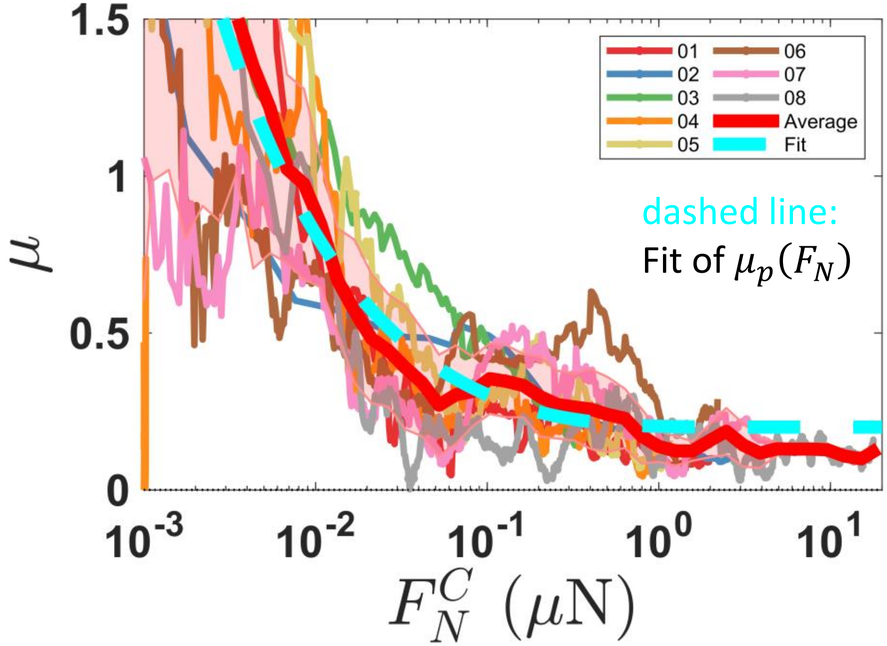

μ_p decreases with increasing F_N.

Fit for the dependence of $\mu_p(F_N)$:

$$\mu_p = 0.2 \coth\left(2.5\, \boldsymbol{F_N}^{0.5}\right)$$

$\mu_p(F_N)$-profile in NaI

NaI solution

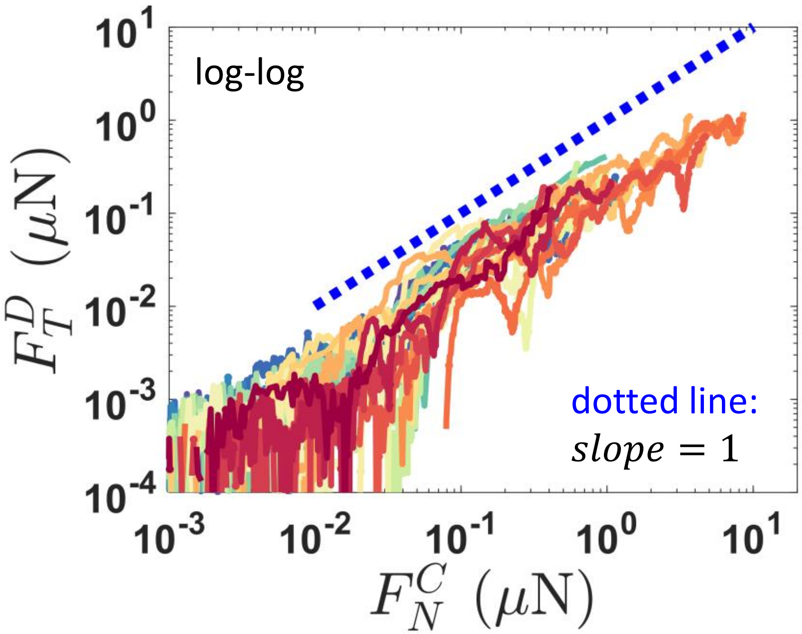

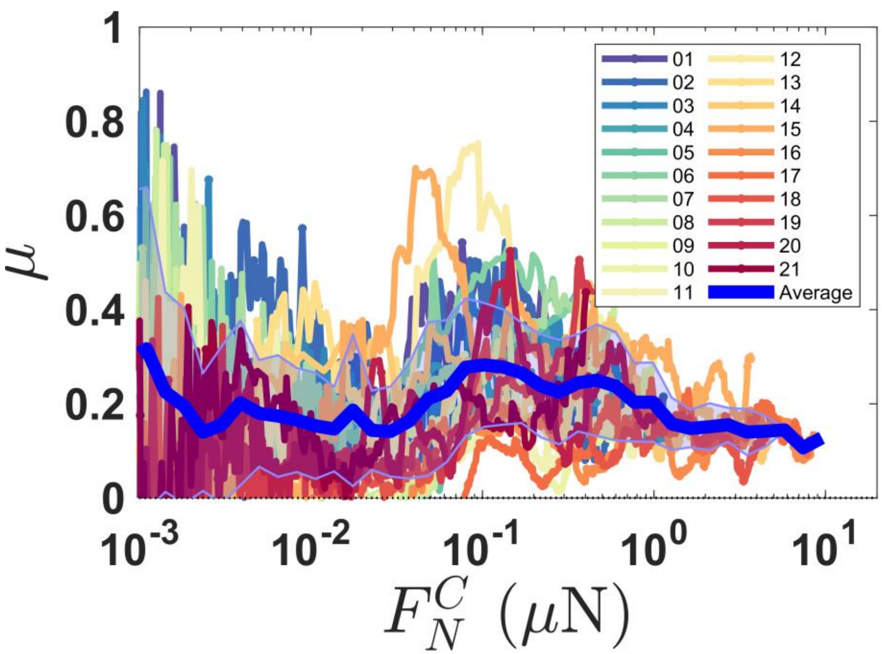

μ_p is constant despite of increasing F_N.

→ The small repulsive forces must have plateaued $\mu_p(F_N)$ profile.

$\mu_p \approx 0.2$.

$\mu_p(F_N)$-variation in PEG

PEG

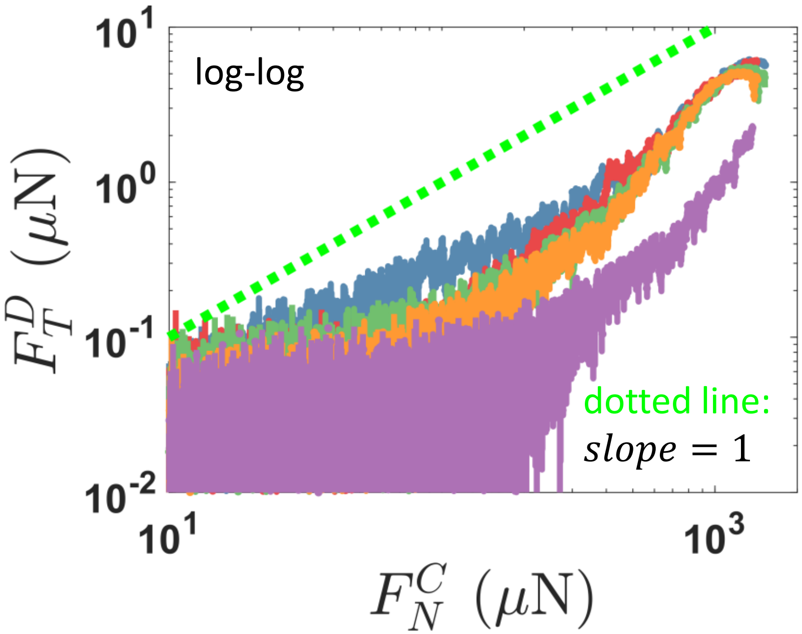

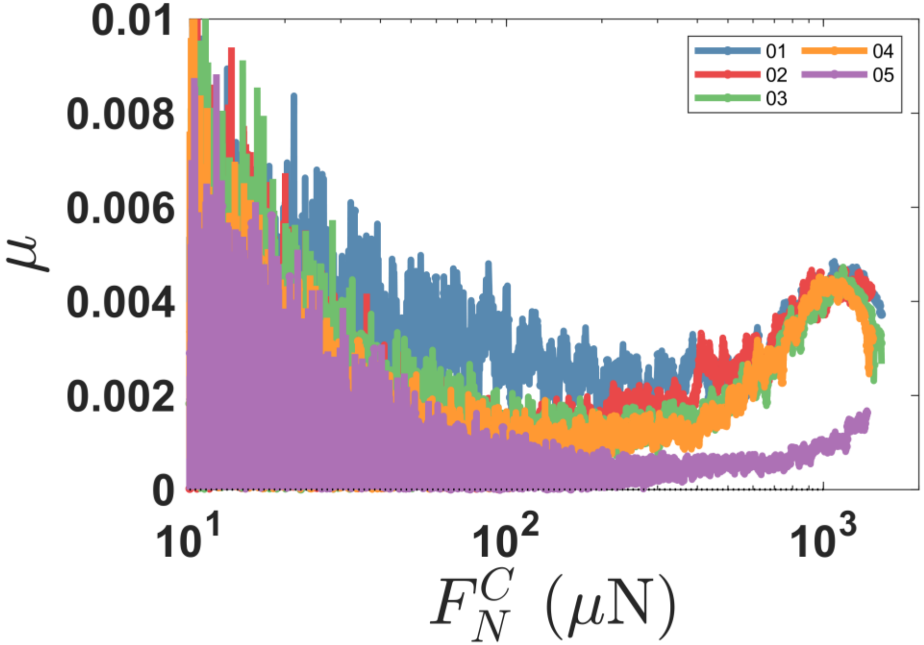

$\mu_p \approx 0$ at all F_N.

Flow curves

NaI solution

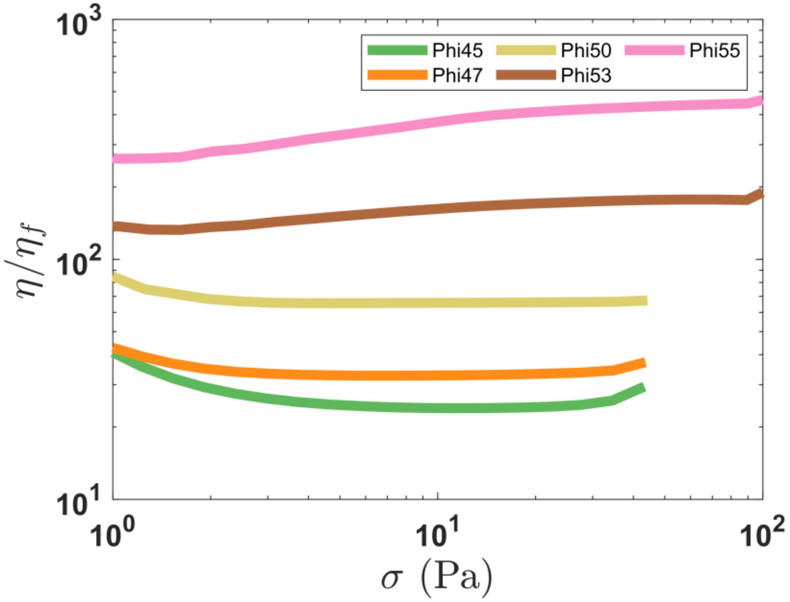

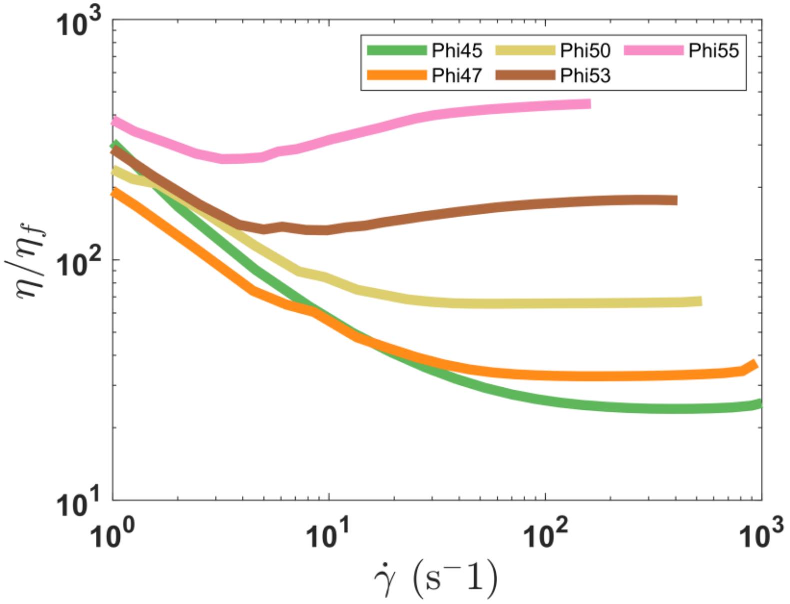

Inertial regime starts from $\dot{\gamma} \approx 3\ s^{-1}$.

In the inertial regime: Newtonian behavior.

Flow curves

PEG, between 2 cross-hatched plates

Old sample (>24h)

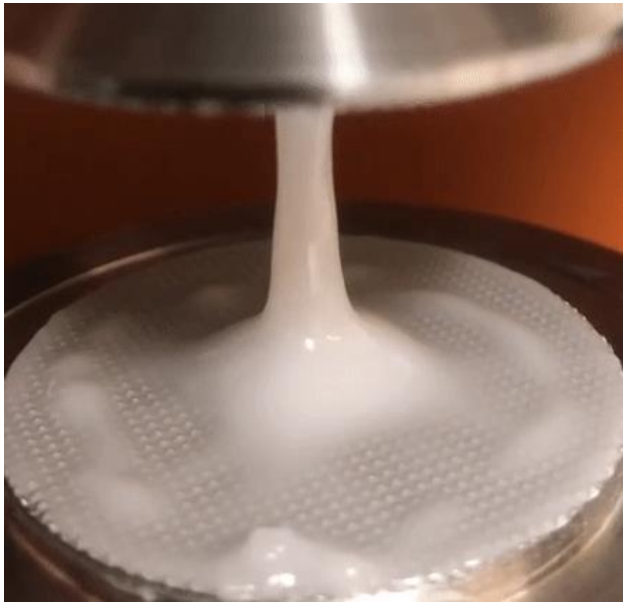

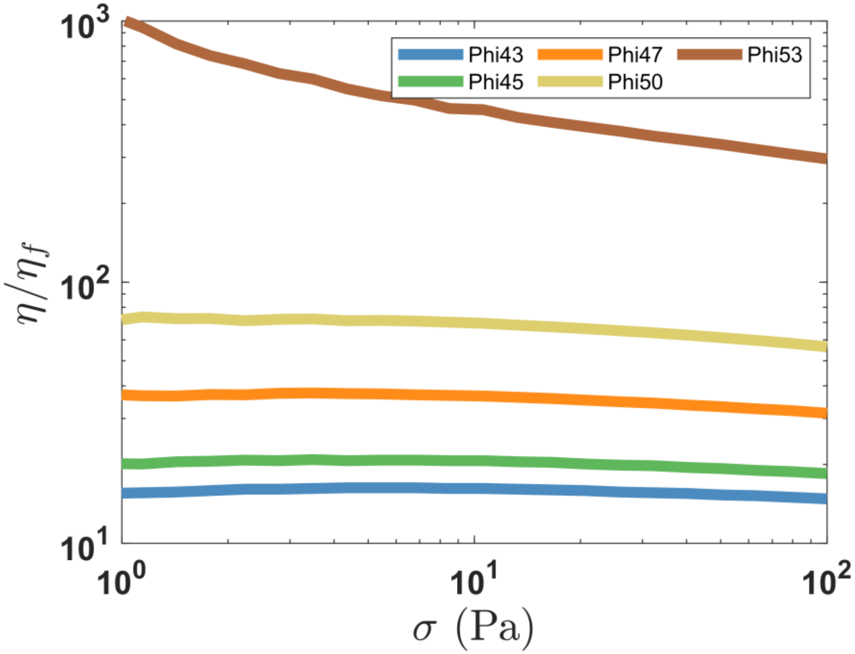

Aged PEG suspension is elastic-like: proof of swelling effect.

Apparent shear thinning: NOT from the variation of μ_p, but from squeezing effect of the shear of the swelled layer.

Results

Flow curves

Silicone oil

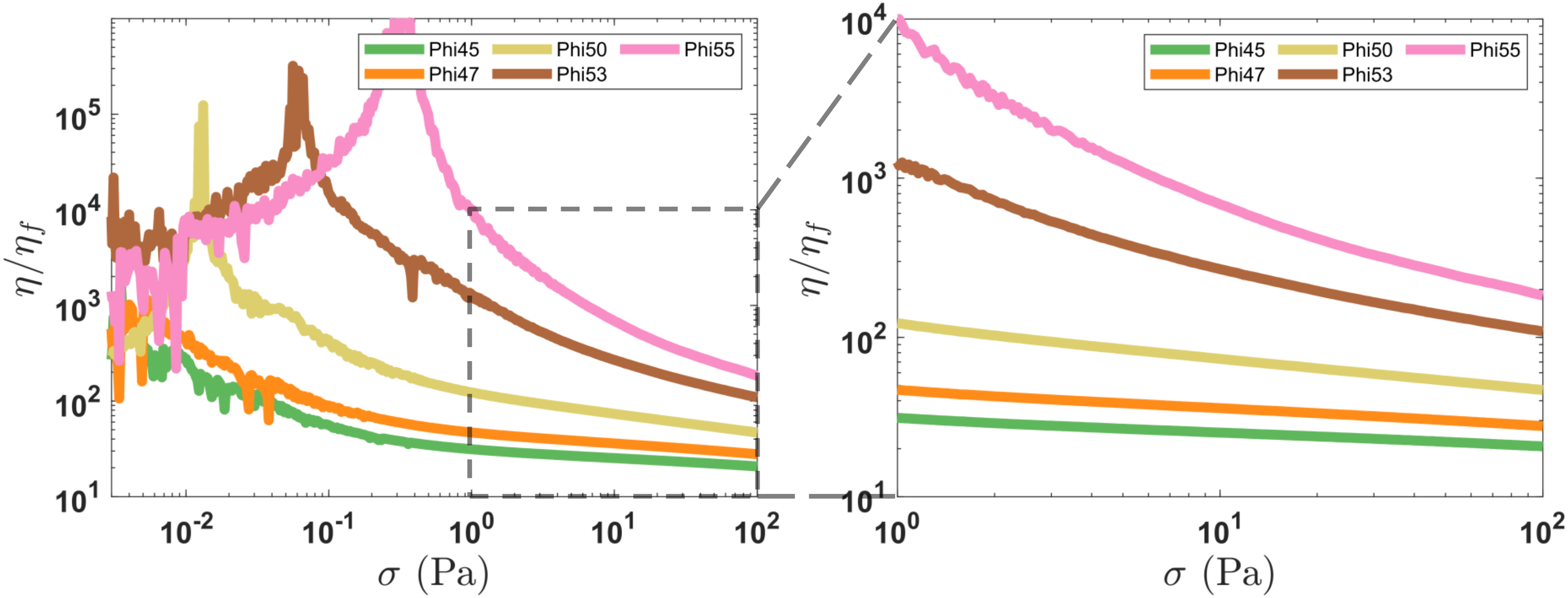

Presence of a small yield stress: quasi-unstable suspension
→data at $\sigma < 10\ \sigma_{\text{yield}}$ are not valid for force analysis.

Shear thinning originates from the reducing of μ_p with F_N.

Rheology vs AFM Si. Oil

From $\eta_s(\sigma)$ and $\mu_p(F_N)$

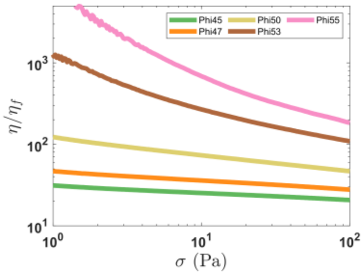

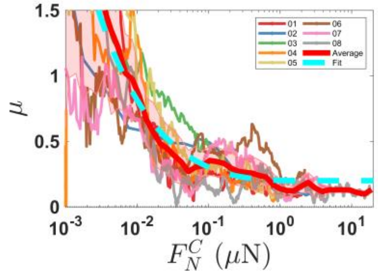

to $\eta_s(\phi)$

showing the dependence ϕ_J on μ_p

Model:

$$\begin{cases} \sigma = \dfrac{1.69\, F_N}{6\pi R^2} \\ \mu_p = 0.2 \coth\left(2.5\, \boldsymbol{F_N}^{0.5}\right) \\ \eta_s(\phi, \mu_p) = \dfrac{\alpha\left(\mu_p(F_N)\right)}{\left(1 - \dfrac{\phi}{\phi_m\left(\mu_p(F_N)\right)}\right)^2} \end{cases}$$

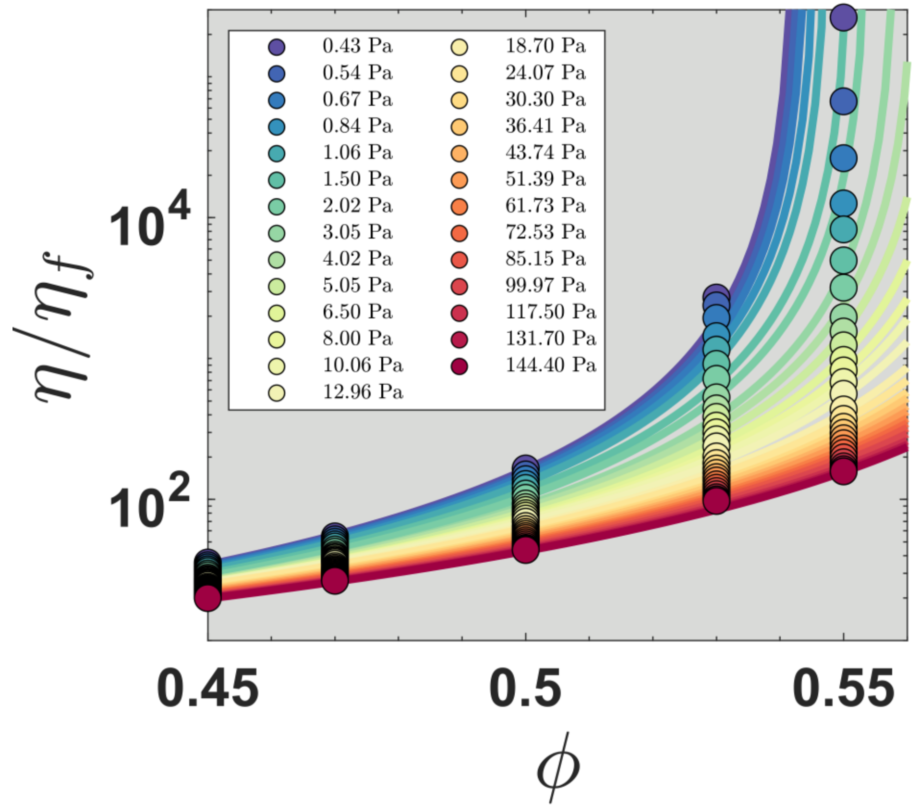

Arshad et al., Soft Matter (2021)

Rheology vs AFM Si. Oil

The dependence of ϕ_m on μ_p

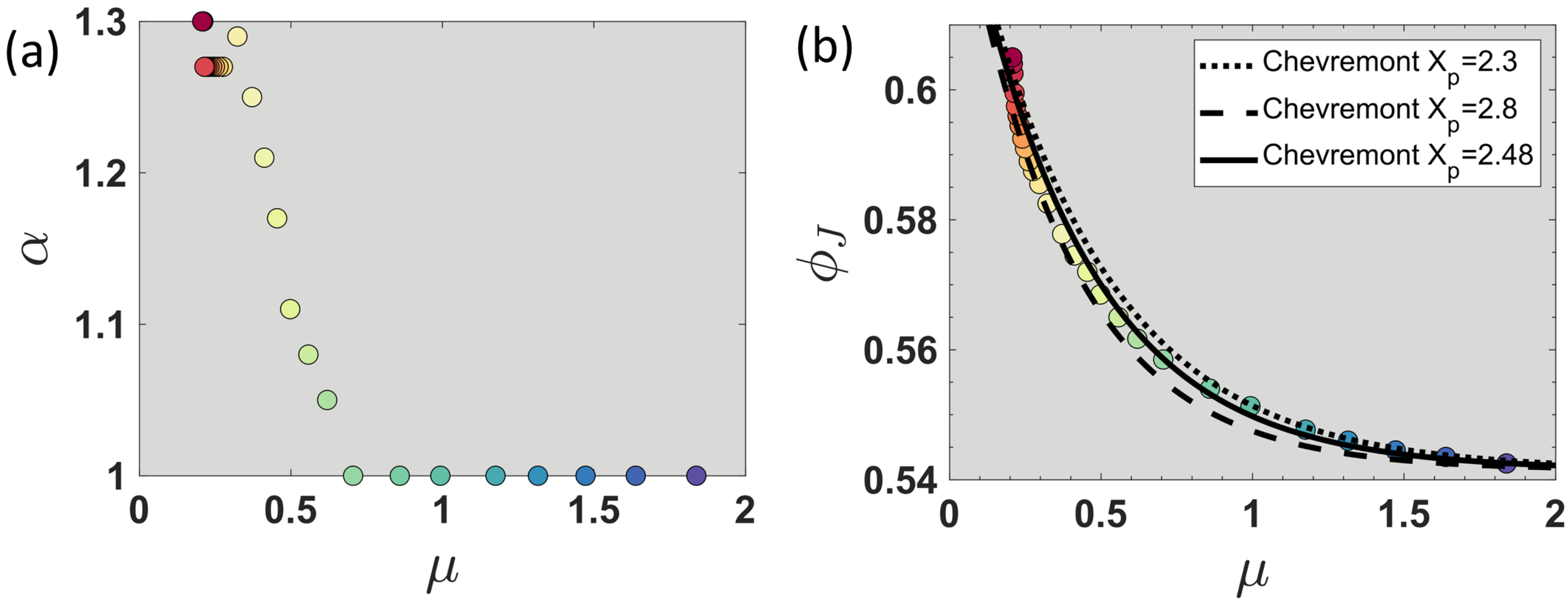

Fit from *Chèvremont et al., PRF (2020)*:

$$\phi_J = \phi_J^{\mu_p=0} - \left(\phi_J^{\mu_p=0} - \phi_J^{\mu_p=\infty}\right)\left[1 - \exp\left(X_p \mu_p\right)\right]$$

with $\phi_J^{\mu_p=0} = 0.64, \phi_J^{\mu_p=\infty} = 0.5415, X_p = 2.8$

Rheology vs AFM PEG

From $\eta_s(\sigma)$ and $\mu_p(F_N)$

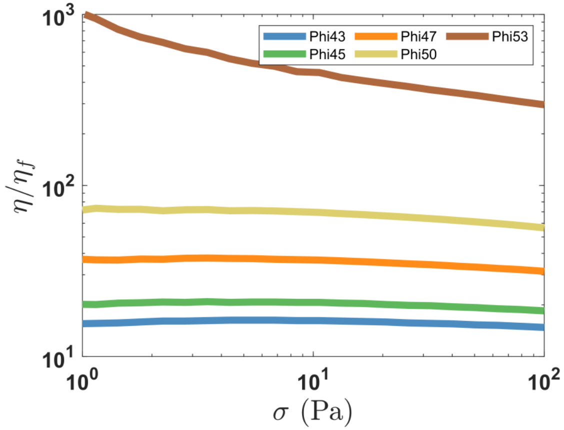

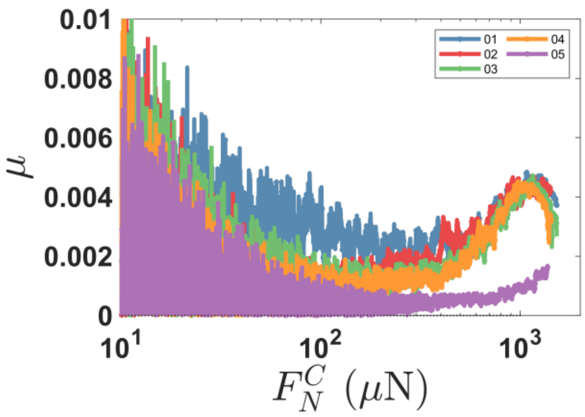

Max shear force = 0.4 N where $\mu_p = 0$

to $\eta_s(\phi)$

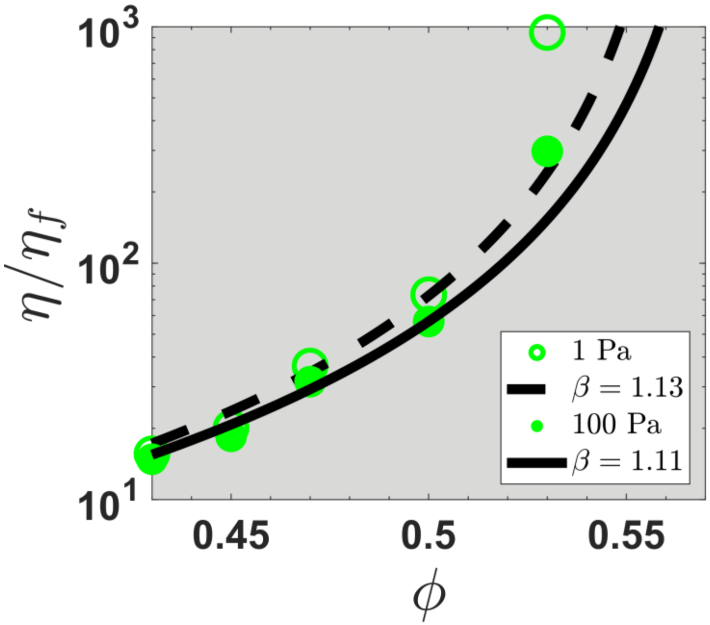

$$\eta_s(\phi, \mu_p) = \frac{1}{\left(1 - \frac{\beta\,\phi}{0.64}\right)^2}$$

High shear stresses reduce β → shear forces squeeze the swelled layer.

Rheology vs AFM NaI sol.

From $\eta_s(\sigma)$ and $\mu_p(F_N)$

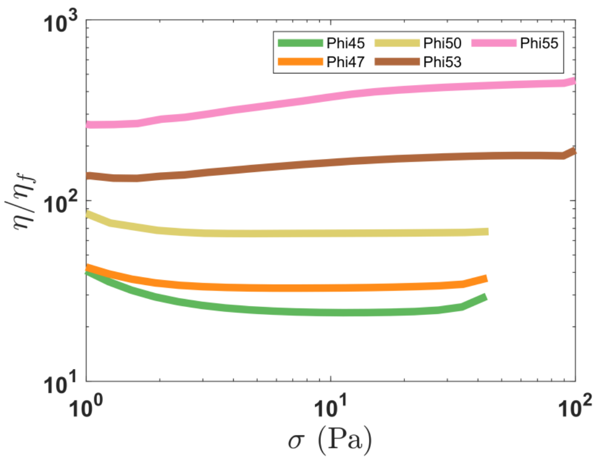

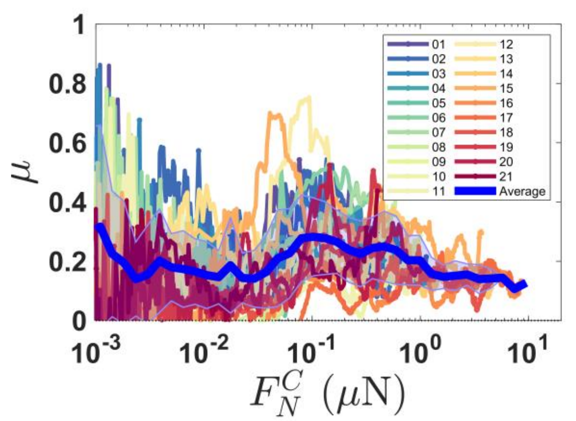

Inertial from the start.

In inertial regime, there is no role of contact.

There is no-known fit for $\eta_s(\phi)$.

Conclusion & Outlooks

Conclusion: the importance of μ_p

Solvents heavily impact the characteristics of particle contact, via F_N^C, F_T^D, and μ_p.

Experimental evidence of the role of decreasing μ_p on shear thinning behavior.

By transitioning from frictionless to inertial regime, shear thickening can occur even without friction.

During the transition from frictionless state to frictional state, dense suspensions flow imhomogeneously in the form of density waves.

Outlooks: Vibrations

Particles force profiles under vibrations:

Will the added vibrations generate repulsive forces before contact?

Will they alter the force profile during contact?

Rheological behaviors under vibrations:

Low amplitude – High frequency for colloidal suspension

High amplitude – Low frequency for granular suspension

Reducing viscosity: What is interplay between vibrations and friction force.

(collaboration with LoF, Bordeaux)

Merci de votre attention!

Methods

Calibration of TFM

Aluminum TF:

Parameters	Normal mode	Tangential mode
Static stiffness k_0	$480000\ \mathrm{N\ m^{-1}}$	$154000\ \mathrm{N\ m^{-1}}$
typical Resonating frequency f_0	$1400\ \mathrm{Hz}$	$700\ \mathrm{Hz}$
typical Q factor Q_0 (in air)	$3000 - 2000$	$600 - 400$
Typical Accelerometer factor C_{accel}	$0.430\ \mathrm{\mu m\ V^{-1}}$	$1.720\ \mathrm{\mu m\ V^{-1}}$
typical Driving factor C_{drive}	$50\ \mathrm{nm\ V^{-1}}$	$100\ \mathrm{nm\ V^{-1}}$
typical Force transduction factor C	$10\ \mathrm{\mu N\ V^{-1}}$	$30\ \mathrm{\mu N\ V^{-1}}$

2 modes are decoupled

$$C = \frac{k_0}{Q_0} C_{\mathrm{drive}}$$

typical Resonance curves:

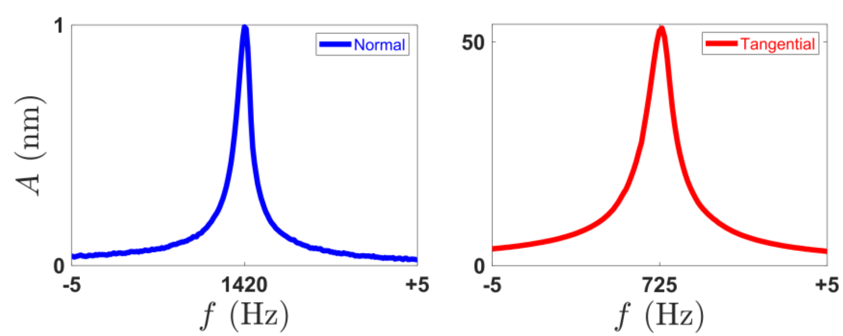

Calibration of TFM

Quartz TF:

Parameters	Normal mode	Tangential mode
Static stiffness k_0	$26630\ \mathrm{N\ m^{-1}}$	$8550\ \mathrm{N\ m^{-1}}$
typical Resonating frequency f_0	$29000\ \mathrm{Hz}$	$16000\ \mathrm{Hz}$
typical Q factor Q_0 (in air)	$3000 - 2000$	$600 - 400$
Typical Accelerometer factor C_{elect}	$50\ \mathrm{nm\ V^{-1}}$	$2950\ \mathrm{nm\ V^{-1}}$
typical Driving factor C_{drive}	$300\ \mathrm{nm\ V^{-1}}$	$300\ \mathrm{nm\ V^{-1}}$
typical Force transduction factor C	$5\ \mathrm{\mu N\ V^{-1}}$	$10\ \mathrm{\mu N}\ V^{-1}$

2 modes are decoupled

$$C = \frac{k_0}{Q_0} C_{\mathrm{drive}}$$

typical Resonance curves:

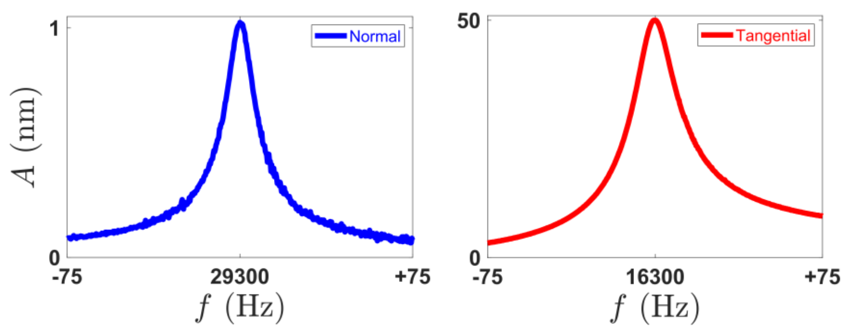

Effect of changing Q and k

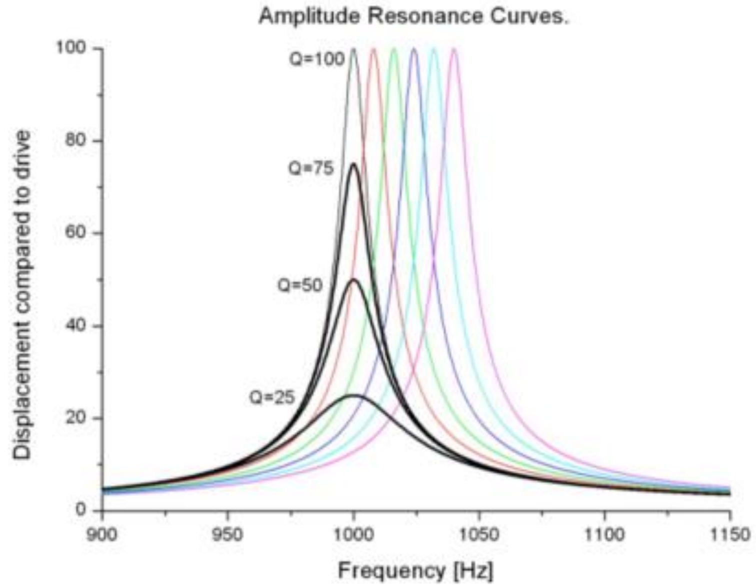

Fig. 2. Amplitude resonance curves for four values of Q (same k) and six values of k (same Q) increasing from left to right.

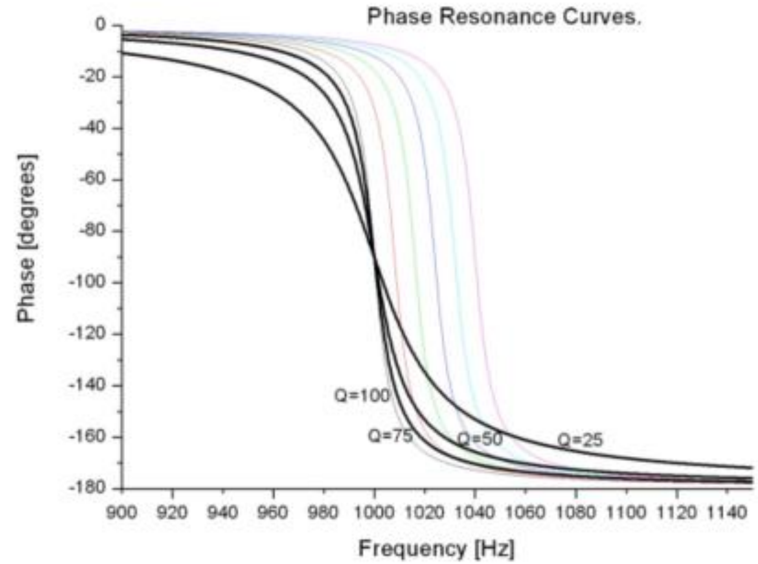

Fig. 3. Phase resonance curves for four values of Q (same k) and six values of k (same Q) increasing from left to right.

METHODS

Principe of PLL

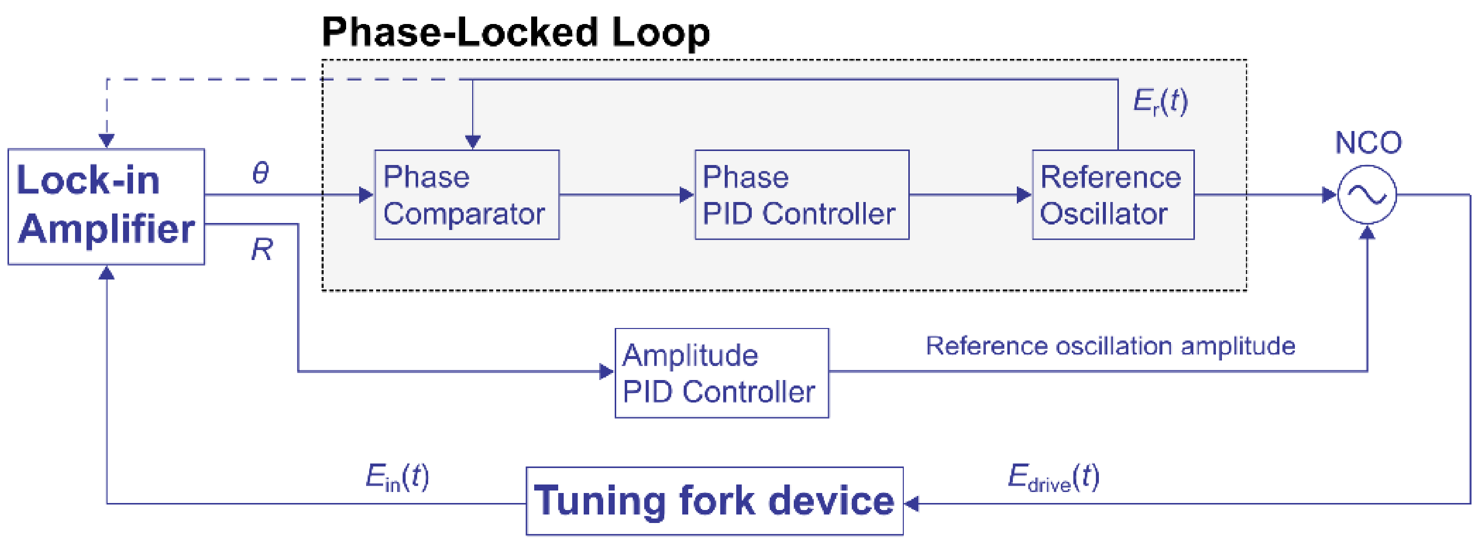

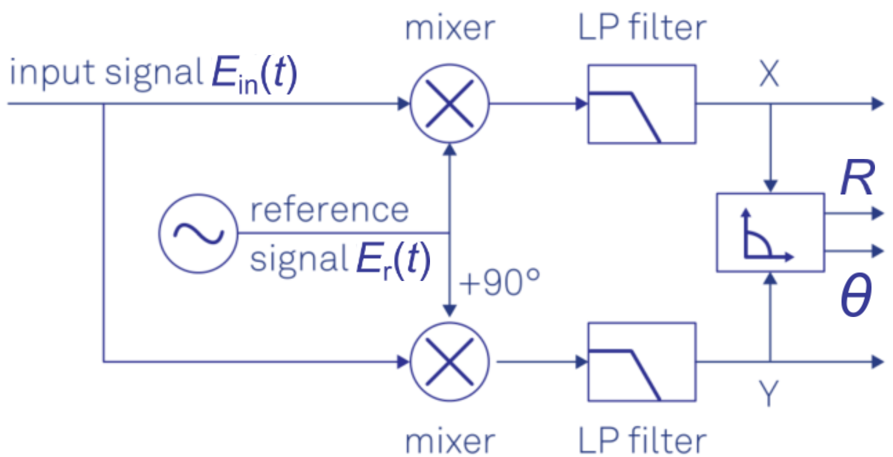

Contact force profiles

Silicone oil

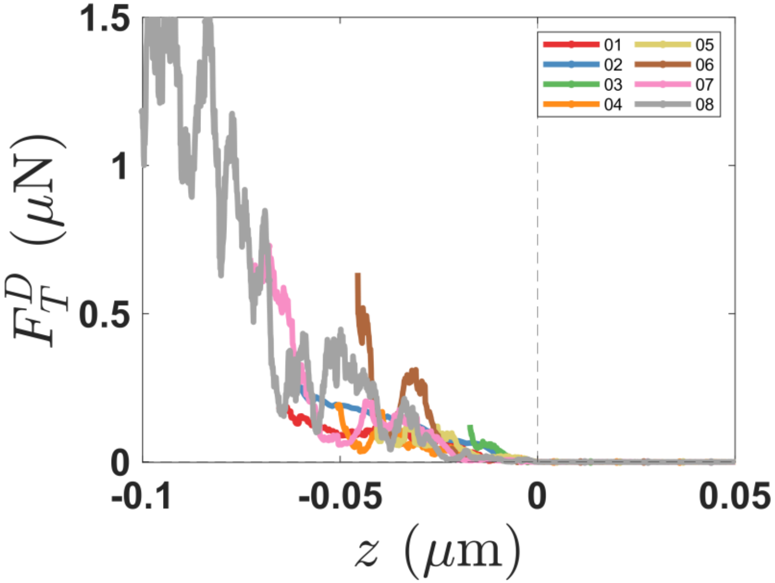

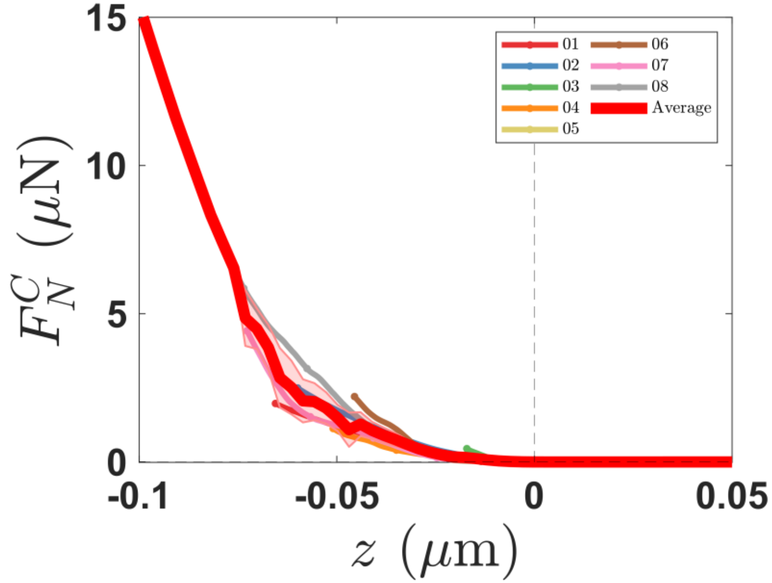

$F_N(z)$ **model:** $F_N^C = f(z, E_0, h_r)$

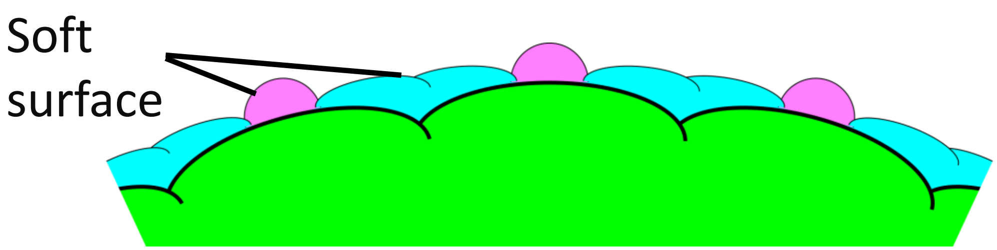

z	E_0	h_r
0 nm - 15 nm	1 GPa	15 nm
15 nm - 50 nm	1 GPa	90 nm
50 nm - center	3 GPa	530 nm

The aims:

Measure Load-dependent variation of Friction coefficient
Compare with the simulation of Lemaire's group

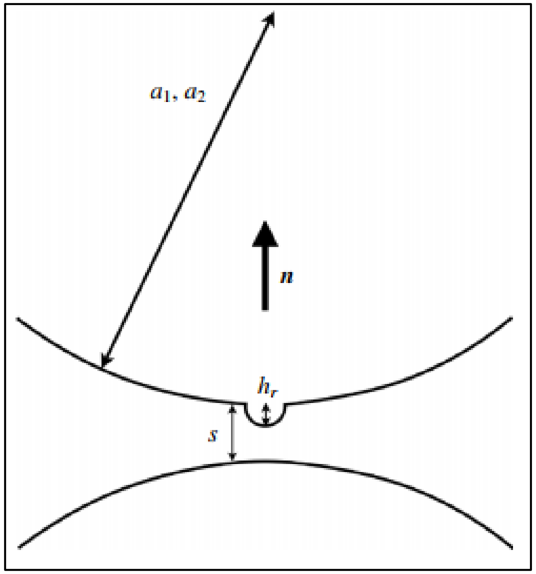

Lobry et al., J. Fluid Mech. (2019)

Contact between a single asperity and a smooth surface

$\boldsymbol{F_N(z)}$ model :

$$\boldsymbol{F}_n = -L_c\left(\frac{\delta}{\delta_c}\right)^{3/2}\left[1-\exp\left(\frac{1}{1-\left(\frac{\delta}{\delta_c}\right)^{\beta}}\right)\right]\boldsymbol{n},$$

Stokes force:

$$\boldsymbol{F_N} = \frac{1}{1.69}6\pi\eta_0\eta_s R^2\dot{\boldsymbol{\gamma}}$$
$$= \frac{1}{1.69}6\pi R^2\boldsymbol{\sigma}$$

with η_0, η_s: fluid viscosity, relative viscosity
L_c, δ_c: critical load and overlap
(which are functions of E_0 and h_r)
E_0: elastic modulus, h_r: asperity height.

Contact force profiles

NaI solution

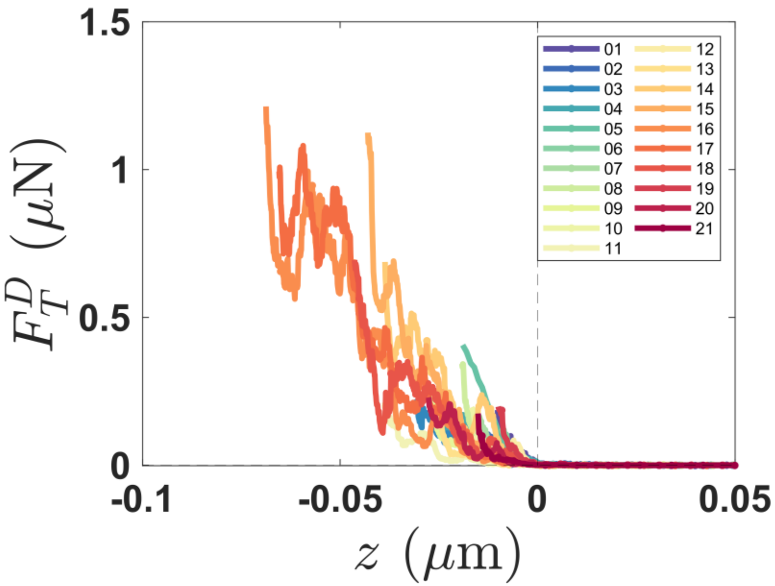

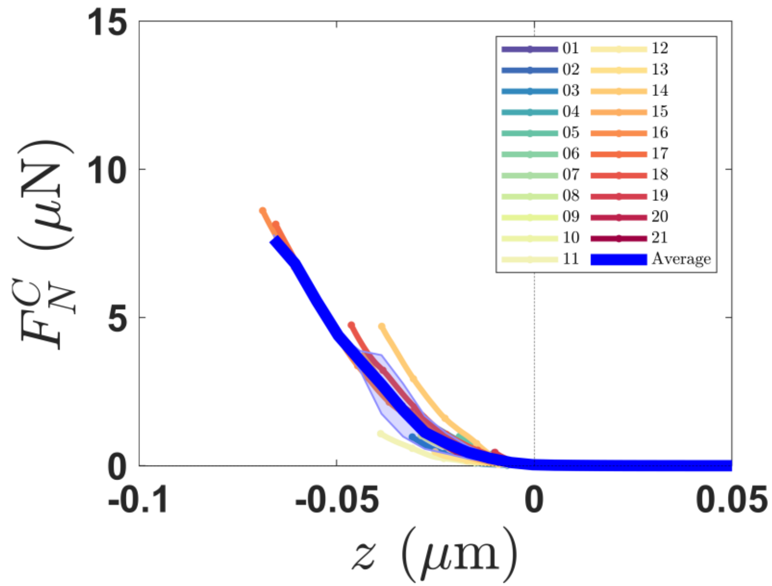

$F_N(z)$ model $F_N^C = f(z, E_0, h_r)$

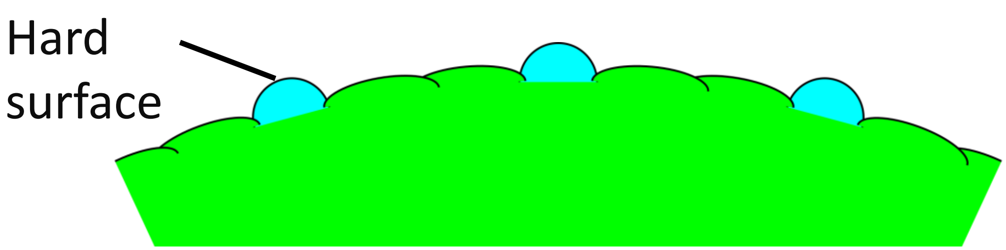

z	E_0	h_r
0 nm - 23 nm	3 GPa	20 nm
23 nm - center	3 GPa	300 nm

RESULTS

Shear reversal

PS particles in Silicone oil

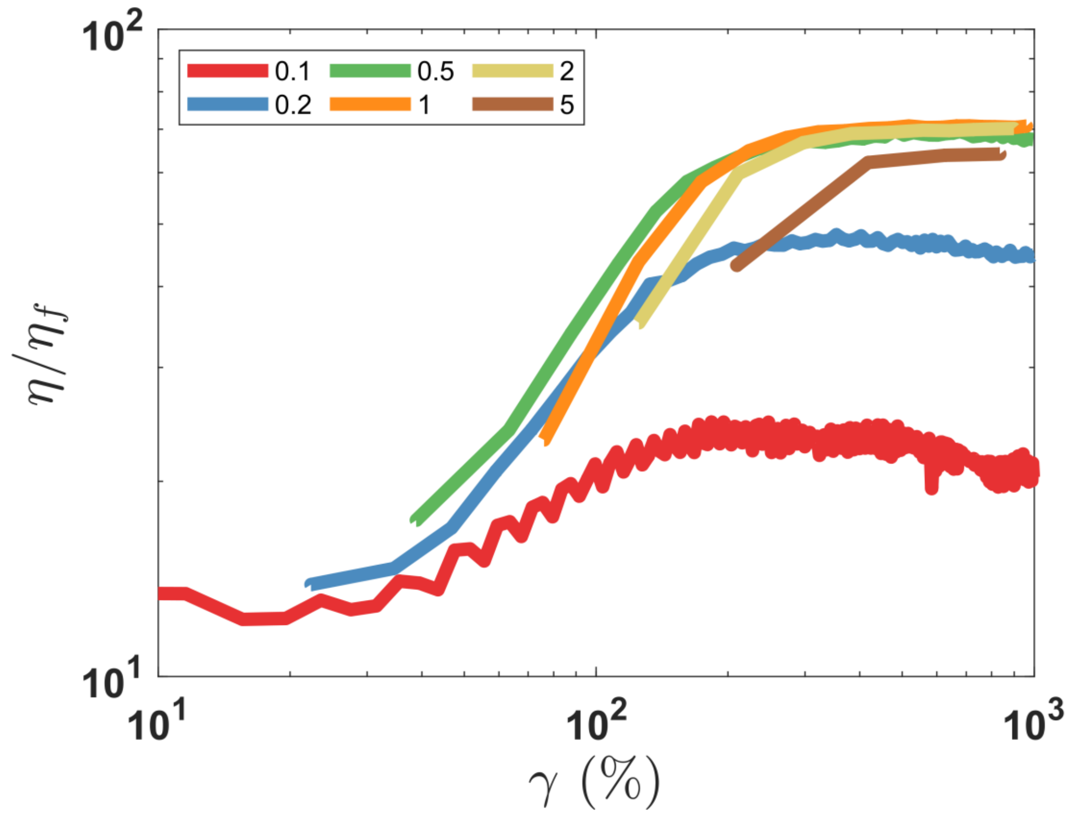

RESULTS
Shear reversal

PS particles in PEG

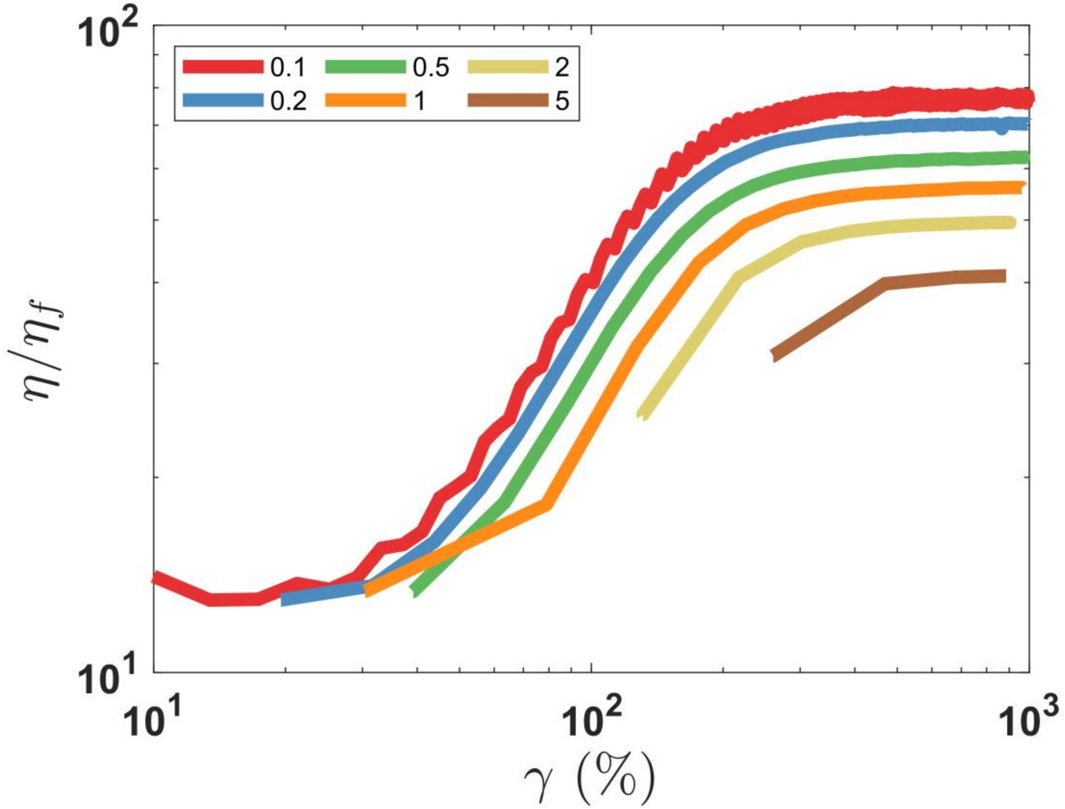

Shear reversal

PS particles in NaI solution

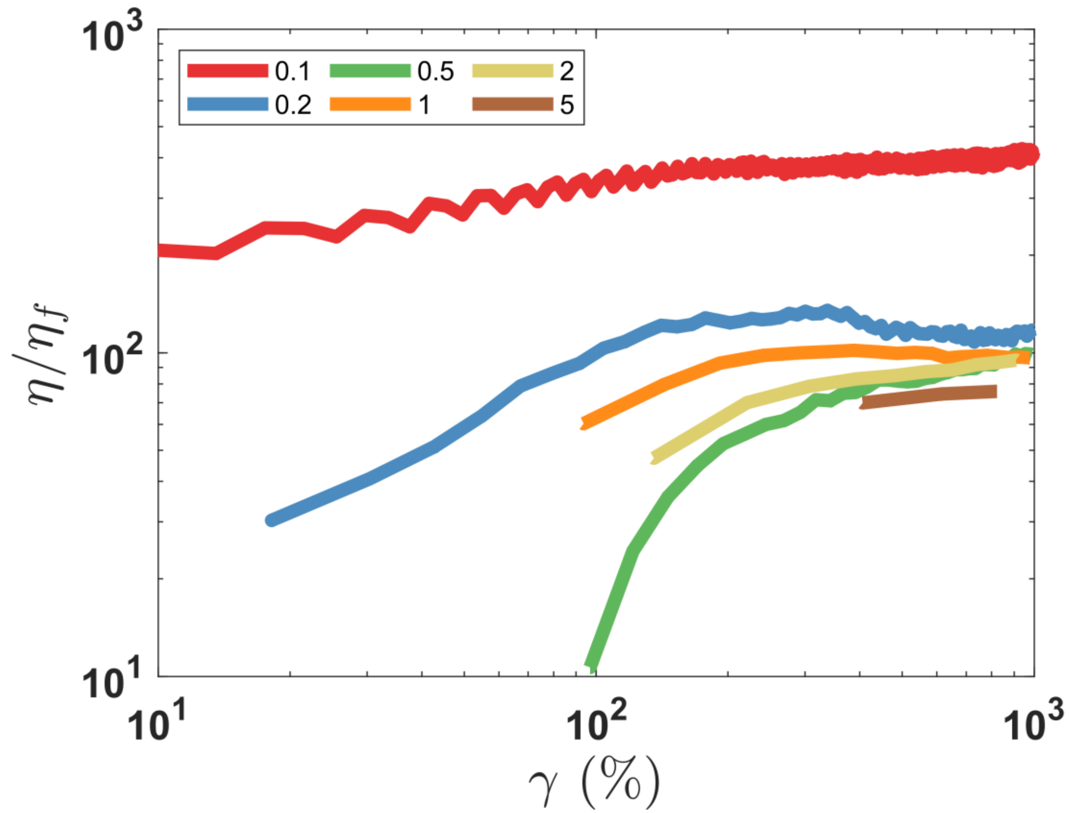

Results

Approach-Retract

PS particles in Silicone oil

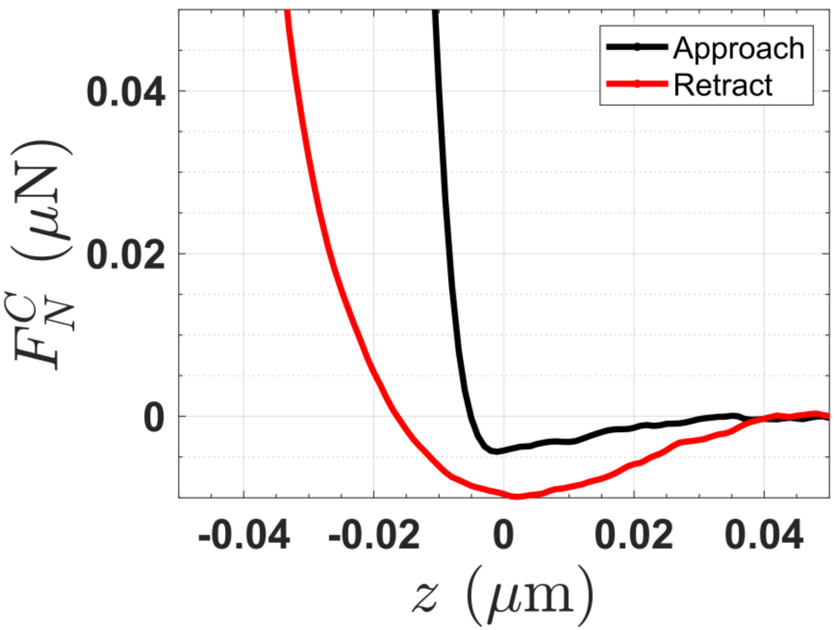

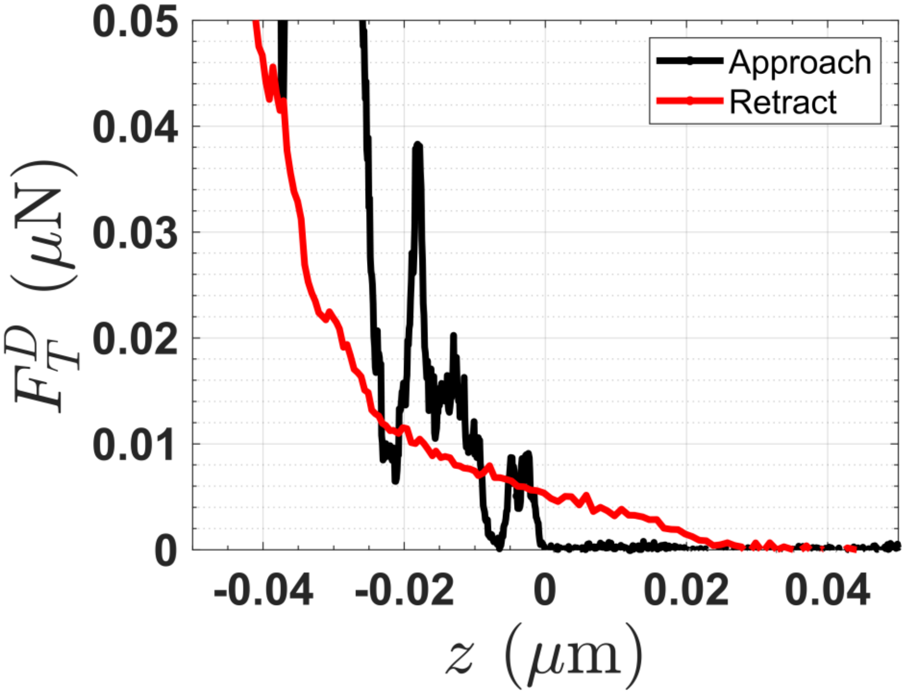

Approach-Retract

PS particles in PEG

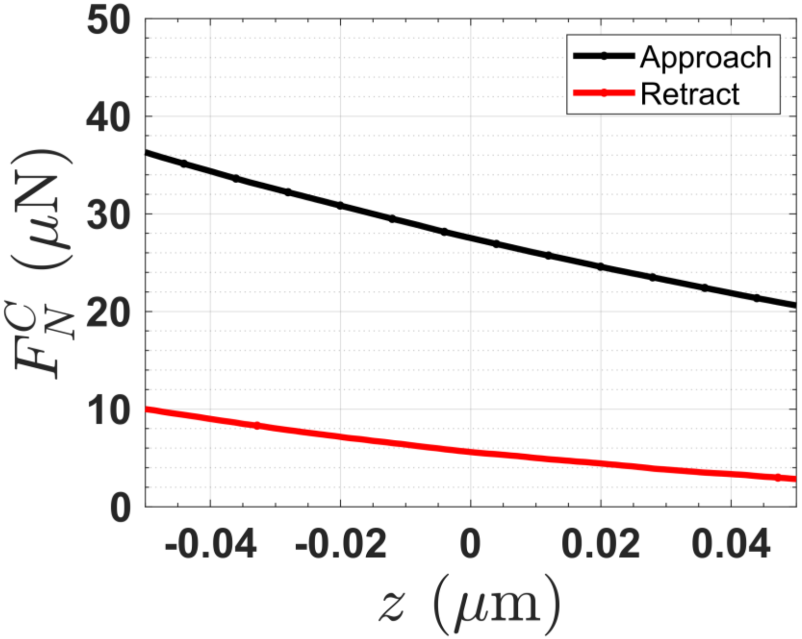

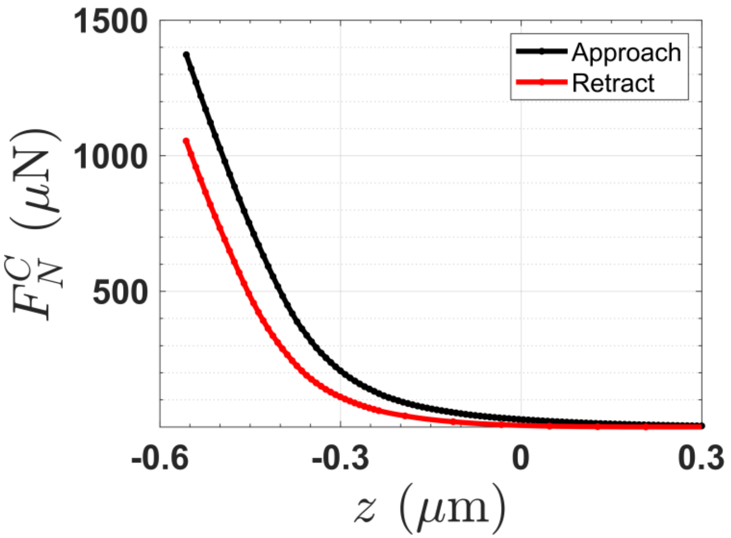

Approach-Retract

PS particles in NaI solution

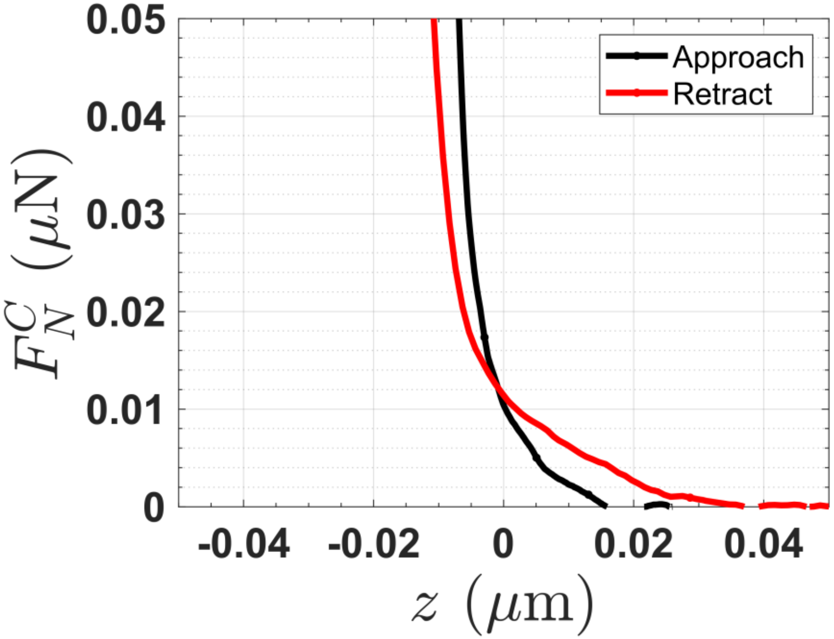

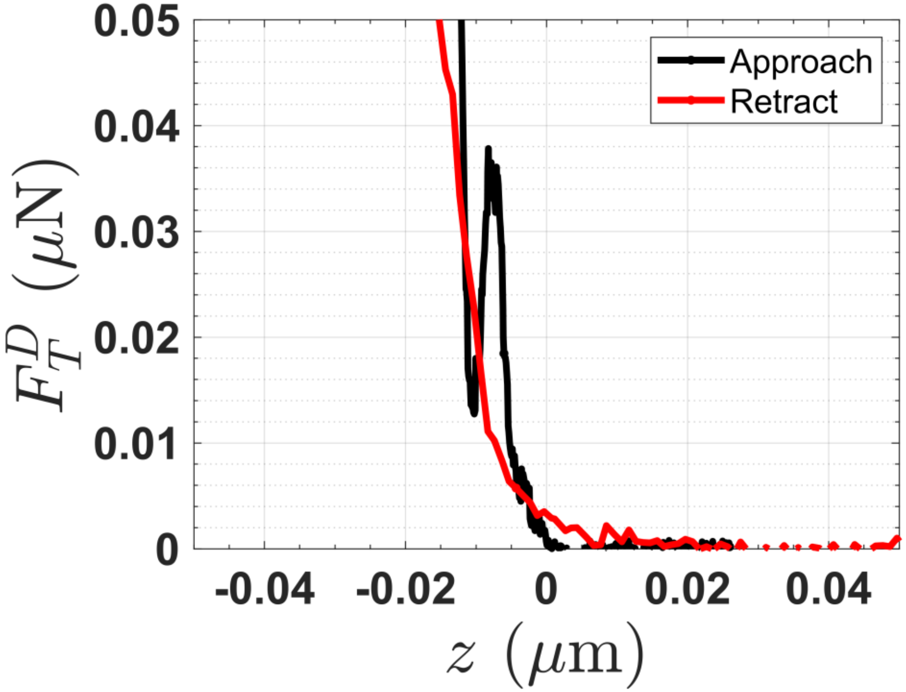

Raw-Clean differences

PS particles in Silicone oils

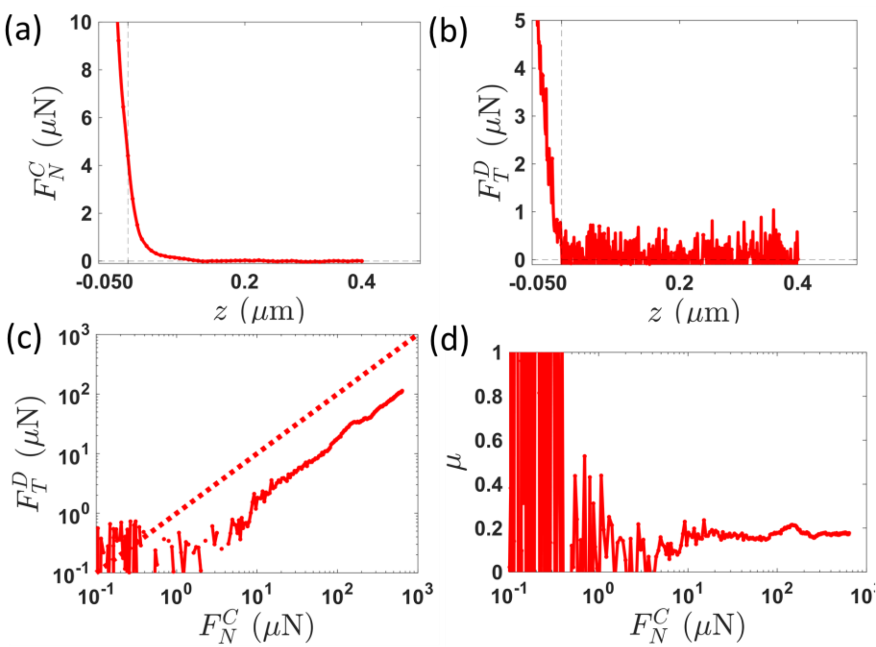

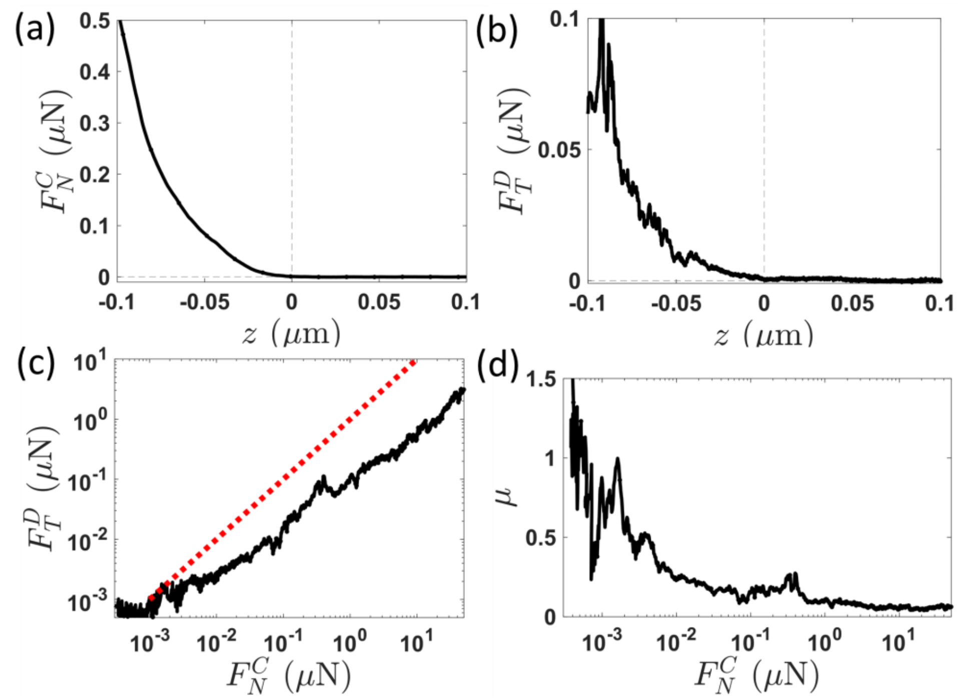

Raw d140 in Oil20

Clean d40 in Oil5

Raw-Clean differences

PS particles in NaI